Universidade do Minho
Escola de Engenharia

Pedro José Ferreira da Silva

Development of a localized drug delivery system with chitosan and ferromagnetic nanoparticles produced by wetspinning for cancer treatment

october 2022

Development of a localized drug delivery system with chitosan and ferromagnetic nanoparticles produced by wetspinning for cancer treatment
Pedro Silva
UMinho | 2022

Universidade do Minho
Escola de Engenharia

Pedro José Ferreira da Silva

Development of a localized drug delivery system with chitosan and ferromagnetic nanoparticles produced by wetspinning for cancer treatment

Master's Dissertation
Integrated Master in Biomedical Engineering
Biomaterials, Rehabilition and Biomechanics

Work developed under supervision of
Doctor Diana Sara Pereira Ferreira
Professor Raul Manuel Esteves Sousa Fangueiro

october 2022

STATEMENT OF INTEGRITY

I hereby declare having conducted this academic work with integrity. I confirm that I have not used plagiarism or any form of undue use of information or falsification of results along the process leading to its elaboration.

I further declare that I have fully acknowledged the Code of Ethical Conduct of the University of Minho.

AGRADECIMENTOS

Assim chega ao fim uma das etapas mais difíceis da minha vida e sem dúvida o ano mais difícil do meu percurso académico. Um ano repleto de muito trabalho e esforço e onde foi preciso ter enorme resiliência.

Com isto, quero agradecer às pessoas que contribuíram para que este ano ainda assim contribuísse para todo o meu crescimento e conhecimento. Antes de tudo quero agradecer aos meus orientadores, ao Professor Raul Fangueiro por disponibilizar todas as condições que fui tendo para a realização do meu trabalho e à Doutora Diana Ferreira pela orientação, disponibilidade e por me ter ajudado a levar sempre este trabalho com o devido rigor, motivação e empenho. Agradecer também a todas as pessoas do 2C2T, Fibrenamics e à Sónia que sempre estiveram lá quando precisei de algo, mostrando total disponibilidade. Para além disto, queria deixar também os meus agradecimentos à Joana, à Sofia e à Marta por todo o apoio, incentivo e ajuda que me foram prestando também ao longo deste ano que foi fundamental para que pudesse concluir o meu trabalho. Sem esquecer, claro, os meus "amigos do lab", do "binde pá festa", o Milhazes e o Gil com quem tive oportunidade de partilhar mais uma vez memórias, risos e desabafos que só nós sabemos o quanto nos tornam mais felizes e o quanto podem melhorar o nosso ano.

Por fim, mas nunca menos importante, à minha família em especial aos meus pais e irmãos e à minha namorada Mariana, por saberem sempre a melhor forma de dizer e fazer as coisas, por mostrarem que independentemente das dificuldades nunca me vão deixar para trás sozinho, por me fazerem ver que nestes momentos precisamos sempre de alguém que mostre que se preocupa, de verdade, e que essas pessoas independentemente da altura do ano ou hora, serão sempre eles, por todo o carinho e incentivo incondicional e por me conhecerem como ninguém, tornando a minha continuidade nos estudos sempre mais fácil de suportar e acabar. Obrigada por tudo o que passou e por tudo o que aí vem! É apenas o começo.

RESUMO

O cancro é uma das principais causas de mortalidade no mundo, depois das doenças cardiovasculares. Assim, há uma necessidade urgente de desenvolver novas estratégias para melhorar a eficácia da prevenção, diagnóstico e tratamento desta patologia.

Uma das terapias estudadas para tal na atualidade é a hipertermia. Este procedimento baseia-se no aumento da temperatura para 40-43 °C do tecido corporal para danificar e destruir as células cancerígenas ou torná-las mais suscetíveis aos efeitos de outras terapias como a radio ou a quimioterapia. Recentemente, e devido aos avanços científicos na área da nanotecnologia, surge o conceito de hipertermia magnética que se baseia na utilização de nanopartículas magnéticas. Apesar das diversas vantagens de utilizar nanopartículas, estas podem apresentar alguma dificuldade em alcançar os tecidos específicos a tratar e, devido ao comum processo de formação de agregados, a sua aplicabilidade pode tornar-se difícil. No sentido de ultrapassar estas limitações, as nanopartículas podem ser incorporadas em sistemas de entrega localizada, nomeadamente compostos por fibras, capazes de atuar como agentes terapêuticos localizados.

Sendo assim, este trabalho teve como objetivo desenvolver novos filamentos por *wetspinning* capazes de serem utilizados na construção e *design* de estruturas fibrosas de entrega localizada de agentes bioativos.

Vários parâmetros da técnica de *wetspinning* foram otimizados para obter os melhores filamentos, sendo que os melhores foram obtidos utilizando uma taxa de fluxo de 1 mL/min, uma agulha de 0.41 mm de diâmetro e um banho de coagulação de 1M de hidróxido de sódio. As fibras obtidas com melhores resultados mecânicos foram produzidas com uma formulação otimizada de 3 %(m/v) de óxido de polietileno com 3 %(m/v) de quitosano em 12 %(v/v) de ácido acético. O banho de *crosslinking* também foi otimizado, sendo que se utilizou um banho de trifosfato de sódio a 1 %(v/v) durante 4 horas. As nanopartículas ferromagnéticas foram então sintetizadas usando o método de co-precipitação e foram introduzidas nas fibras em diferentes percentagens. Os filamentos funcionalizados com 2 %(m/v) de nanopartículas mostraram o melhor desempenho mecânico, melhorando também a estabilidade estrutural do sistema ao longo do tempo.

Palavras-chave: Fibras, Hipertermia, Nanopartículas Ferromagnéticas, Sistema de Entrega de Fármacos Localizado, *Wetspinning*

ABSTRACT

Cancer is one of the leading causes of mortality in the world, after cardiovascular diseases. Thus, there is an urgent need to develop new strategies to improve the effectiveness of prevention, diagnosis and treatment of this disease.

One of the therapies currently being studied for this is hyperthermia. This procedure is based on increasing the temperature to 40-43 °C of the body tissue to damage and destroy cancer cells or make them more susceptible to the effects of other therapies such as radio or chemotherapy. Recently, and due to scientific advances in nanotechnology, the concept of magnetic hyperthermia has emerged, which is based on the use of magnetic nanoparticles. Despite the several advantages of using nanoparticles, these may present some difficulty in reaching the specific tissues to be treated and, due to the common process of aggregate formation, their applicability may become difficult. In order to overcome these limitations, nanoparticles can be incorporated into localized delivery systems, namely composed of fibres, capable of acting as localized therapeutic agents.

Therefore, this work aimed to develop new filaments by wetspinning that can be used in the construction and design of fibrous structures for localized delivery of bioactive agents.

Several parameters of the wetspinning technique were optimized to obtain the best filaments, and the best ones were obtained using a flow rate of 1 mL/min, a 0.41 mm diameter needle, and a 1M sodium hydroxide coagulation bath. The fibres obtained with the best mechanical results were produced with an optimized formulation of 3 %(w/v) polyethylene oxide with 3 %(w/v) chitosan in a 12 %(v/v) acetic acid aqueous solution. The crosslinking bath was also optimized, and a 1 %(v/v) sodium triphosphate bath was used for 4 hours. Ferromagnetic nanoparticles were then synthesized using the co-precipitation method and were introduced into the fibres in different percentages. The filaments functionalized with 2 %(w/v) nanoparticles showed the best mechanical performance, also improving the structural stability of the system over time.

Keywords: Drug Delivery System, Ferromagnetic Nanoparticles, Fibres, Hyperthermia, Wetspinning.

Table of Contents

List of Figures

List of Tables

LIST OF ABBREVIATIONS AND ACRONYMS

AcOH – Acetic acid

ATR-FTIR - Attenuated Total Reflectance - Fourier Transform Infrared Spectroscopy

BBR - Berberine

CH - Chitosan

DNA - Deoxyribonucleic acid

DOX - Doxorubicin

EDS - Energy Dispersive X-Ray Spectroscopy

ES - Electrospinning

FESEM - Field Emission Scanning Electron Microscopy

FDA - Food and Drug Administration

GTA - Glutaraldehyde

IARC - International Agency for Research on Cancer

MNPs - Magnetic Nanoparticles

MIONs - Magnetic Iron Oxide Nanoparticles

MRI - Magnetic Resonance Imaging

NaOH – Sodium hydroxide

NPs - Nanoparticles

PEO - Poly(Ethylene Oxide)

PVA - Poly(vinyl alcohol)

PVAc - Poly(vinyl acetate)

ROS - Reactive oxygen species

SEM - Scanning Electron Microscope

STEM - Scanning Transmitted Electron Microscopy Detector

TGA - Thermogravimetric Analysis

TPP - Sodium tryphosphate

VCM - Vancomycin

WS - Wetspinning

XRD - X-ray Diffraction

1 INTRODUCTION

1.1 CONTEXT AND MOTIVATION

Cancer incidence and mortality is increasing worldwide, with estimated 19.3 million new cases and 10 million cancer deaths in 2020, according to the International Agency for Research on Cancer (IARC) [1].

Malignant tumors become more heterogeneous as they develop, resulting in a mixed population of cells with varying molecular characteristics and receptivity to therapy. This variability may be seen at both the geographical and temporal levels, and it is the driving force behind the formation of resistant phenotypes induced by a selection pressure during cancer treatment [2]. Thus, finding novel strategies to improve the therapy efficiency while minimizing the side effects is crucial [3].

Hyperthermia is a cancer therapy and is regarded to be an artificial means of increasing body tissue temperature by administering heat from external sources to destroy malignant cells or inhibit their further growth. One advantage of employing hyperthermia for cancer treatment is that the use of radiation or chemotherapy medications can be reduced. Furthermore, certain versions of the treatment do not involve surgery and have less side effects [4]. Although, a key drawback of traditional hyperthermia is that both malignant and non-malignant cells are equally susceptible to heating, which can cause substantial issues for healthy cells [5][6].

As a consequence, there has been a great deal of interest in the concept of biologically targeted magnetic hyperthermia, in which targeted magnetic iron oxide nanoparticles (MIONs) are used to increase the temperature in tumors 'site under an alternating magnetic field [7].These nanoparticles (NPs) are used for various biomedical applications and a have multifunctional role in therapeutics, diagnostics, imaging, and drug delivery due to their excellent properties such as chemical stability, non-toxicity, biocompatibility, high saturation magnetization and high magnetic susceptibility [8].

In order to target the required area, drug delivery systems have been used. A drug delivery system is defined as a formulation or a device that enables a therapeutic substance to selectively reach its site of action without reaching the nontarget cells, organs, or tissues [9]. To design intelligent drug delivery the use of biocompatible materials and the design of stimuli-responsive systems are required [8][9].

Wetspinning (WS) is a relatively simple and scalable method to manufacture drug delivery systems. This technique also allows the selection of suitable materials from non-biodegradable to

biodegradable polymers, with the purpose of achieving control over the release profile through diffusion or diffusion and fibre degradation. From the different available materials, chitosan (CH) is preferred as it is a biopolymer that may be used to create unique features, functions, and applications in the biomedical field mostly employed because of its biocompatibility, biodegradability, and non-toxicity. Polyethylene oxide (PEO) is also an exceptionally biocompatible and biodegradable polymer that has the ability to interact with polarized surfaces and is frequently affordable, making it an intriguing biomaterial [10][11]. Poly(vinyl alcohol) (PVA) can also be used, since it is a polymer that has good film forming and physical properties, high hydrophilicity, processability, biocompatibility and good chemical resistance [12][13].

So, in this case, the localized drug delivery system will be based on fibrous structures produced by WS with biocompatible polymers, like CH, PEO and PVA [14][15]. Iron (II,III) oxide (Fe_3O_4) NPs will be synthesized and incorporated into the fibres in different percentages.

Therefore, the development of localized drug delivery systems based on fibrous structures produced by WS, using biodegradable polymers and ferromagnetic NPs, can be a promising strategy to treat cancers by hyperthermia.

1.2 OBJECTIVES

The main objective of this work was to develop a localized drug delivery fibrous system with ferromagnetic NPs using the WS process with possible application in the treatment of cancer by magnetic hyperthermia. Firstly, an optimization process was performed in order to obtain defect-free CH, CH/PEO and CH/PVA fibres by WS. For this, diverse formulations based on CH, CH/PEO and CH/PVA as well as different WS parameters were evaluated. The produced fibres were characterized using different techniques, such as Optical Microscopy, Field Emission Scanning Electron Microscopy (FESEM), Attenuated Total Reflectance - Fourier Transform Infrared Spectroscopy (ATR-FTIR), Thermogravimetric Analysis (TGA), Scanning Transmitted Electron Microscopy Detector (STEM) and Energy Dispersive X-Ray spectroscopy (EDS).

After optimization of the polymeric formulations to obtain the fibres and their characterization, the NPs were synthesized and incorporated into the optimized polymeric formulations to produce fibres with ferromagnetic NPs. These results were characterized using techniques such as ATR-FTIR, TGA, Optical Microscopy, FESEM. Mechanical properties and fibres swelling and degradation were also analyzed.

Finally, the fibres that presented better properties were used for the development of a fibrous structure with magnetic properties that was also fully characterized with the techniques enunciated before as a possible application as a localized therapeutic system for cancer by magnetic hyperthermia.

1.3 STRUCTURE OF THE DISSERTATION

This dissertation is divided into six sections: section 1 contains a brief introduction to the subject under study; section 2 covers the state of the art of the topic under consideration; section 3 contains all the materials and methods used in the development of the dissertation; section 4 presents the results obtained as well as their discussion; section 5 illustrates the main conclusions of the developed work and section 6 contains proposals for future work.

In the first section, a topic framework was created, and the key inspirations that led to this effort, as well as the main objectives of the proposed work, are given. This chapter also includes a synopsis of the content of each part.

Section 2 includes a thorough literature review that takes into account: cancer therapies, with a primary focus on hyperthermia; localized drug delivery systems; the wetspinning technique; the biodegradable polymers used in the production of fibres by this technique and a survey of the work done using the polymers under study and framed in tissue of hyperthermia treatment applications.

Section 3 describes the materials and methodologies that served as the foundation for the experimental execution of this dissertation, as well as the various approaches employed to optimize the five polymeric systems. This chapter also examines and describes the many methodologies utilized for system characterization established during this effort.

Section 4 presents and discusses the findings achieved for each of the created materials. The various optimization phases are correctly presented, both in terms of formulation parameters and wetspinning parameters, demonstrating their effect on the morphology of the generated fibres. Finally, the characterization studies done on the various samples developed in this work are provided.

Section 5 summarizes the study's general results and section 6 outlines possible future possibilities that take into consideration the potential of this application.

2 State Of Art

2.1 CANCER THERAPIES

Cancer is a vast category of illnesses that can begin in practically any organ or tissue of the body when abnormal cells develop uncontrolled, invade neighboring tissues, and/or spread to other organs. The latter phase is known as metastasizing, and it is a primary cause of cancer mortality. Cancer is also known as a neoplasm and a malignant tumor. Normally, human cells grow and multiply to form new cells as the body needs them. In also normal cases, when cells grow old or become damaged, they die, and new cells take their place [16]. However, sometimes this orderly process breaks down and abnormal or damaged cells (cancer cells) grow and multiply, raising the opportunity for tumors to appear. These cells develop because of multiple changes in their genes, which can have many possible causes like lifestyle habits, genes or being exposed to cancer-causing agents.

Once these cells tumors appear, they can expand, owing to their increased vascularization, and spread to other parts of the body, resulting in metastasis and death [17].

In order to fight these diseases, some therapies for cancer are being used. These treatments change depending on the type of cancer being treated and whether it is at an advanced stage or not. Some cancer patients will only receive one therapy to fight this disease, however, the majority of patients will receive a combination of therapies, searching for immediate results, such as surgery along with chemotherapy and radiation therapy [15].

Table 1 shows the mainly strategies in use today and a brief description of them:

Table 1: Most used therapies for cancer treatment

Type of treatment	Description
Photodynamic Therapy	This therapy involves the use of a photoactive molecule, light and molecular oxygen present in tissues. When combined, these three compounds are able to produce reactive oxygen species (ROS), which will induce the death of target cells [18]–[20];
Immunotherapy	This therapy is made up of white blood cells as well as lymphatic organs and tissues. As known, the immune system helps the body fight infections and diseases, and, therefore, this type of cancer treatment helps immune system fight cancer [21];
Endocrine therapy	Cancer treatment that slows or prevents the proliferation of cancer cells that need hormones to proliferate [22];
Surgery	Procedure in which a surgeon tries to remove tumors from a patients' body [23];
Chemotherapy	Treatment that employs strong chemicals to destroy rapidly developing cells in the body [24];
Radiation therapy	Therapy where strong doses of radiation are used to destroy cancer cells and reduce tumors [25];
Hyperthermia therapy	Treatment in which body tissue is heated to temperatures between 40 - 43°C [26] in order to harm and destroy cancer cells [27];

Although certain cancer therapies are still available, most of them have significant drawbacks that make the treatment dangerous. The photodynamic therapy, although a promising treatment, has been performed in only a reduced number of patients, so many clinics don't adopt this type of treatment. Furthermore, with systemically administered photosensitizers, skin photosensitivity is one of the most common adverse events. Patients must avoid sunlight and strong artificial light for weeks, which is usually highly undesirable. Others adverse events often reported are pain and the decreasing efficacy of photodynamic therapy for larger lesions. Besides that, due to inadequate tissue penetration of light, bulky or deep seated tumors are difficult to treat, showing the limitations on this therapy [18].

Regarding immunotherapy, current anticancer immunotherapies have increased overall survival in several cancers at various stages of development, including metastatic disease. In contrast, certain malignancies, create immunosuppressive microenvironments marked by elevated expression of immune checkpoint molecules, reduced tumor antigen expression, and restricted infiltration of circulating immune effector cells. These non-immunogenic, non-inflamed ("cold") tumors respond poorly to immunotherapies and successfully avoid anticancer immune responses which can lead to problems. Additionally, immunotherapy can harm organs and systems due to some of the drugs used on it and also could take longer to work than other treatments [28].

Although there are reports of successful cancer treatment with hormone therapy, this therapy is usually never used without the combination of another, as hormone therapy only attempts to extend "control" over the stage of cancer. Allied to the use of this therapy are side effects that can disrupt the daily life of the patient in question. Some organs may be damaged and the patient may suffer side effects of the administered hormones such as: hot flashes, weight gain and muscle loss, breast swelling and tenderness, fatigue, irritability and also anemia, increased risk of cardiovascular disease (infarction) and increased risk of a metabolic syndrome which may cause concern for those involved [29].

Regarding surgery, the method is never easy and there are cases where it cannot be performed. In situations when it can be used, there is a chance that the cancer will not be entirely eradicated and for that same reason there is a risk that it will spread from its original position to other parts of the body, leading to metastasis. Furthermore, there are secondary dangers like as bleeding, tissue and organ damage, pain, and poor recovery of other body functions that are not well perceived by the patients in question [30].

It is known that chemotherapy may shrink the cancer enough or slow down its growth to make surgery to remove the cancer possible. However, for this to be functional, there are parameters which must be taken into account and which must be studied, such as: the drug uptake and the intracellular

activation of the effective drug. As it is a systemic therapy, not localized, this therapy induces the death of cancerous cells and also the death of healthy cells, which induce many side effects, including fatigue, sickness, loss of appetite and hair and even blood clots [31].

Regarding radiation therapy, the radiation used is called ionizing radiation because it forms ions (electrically charged particles) and deposits energy in the cells of the tissues it passes through. This deposited energy can kill cancer cells or cause genetic changes resulting in cancer cell death. High-energy radiation damages genetic material (deoxyribonucleic acid- DNA) of cells and thus blocking their ability to divide and proliferate further. Nevertheless, this radiation does not kill cancer cells right away, it can take days or weeks of treatment before DNA is damaged enough for cancer cells to die and there's the possibility of also damaging normal cells as well. Beyond that, the equipment is expensive, which leads to a high cost of the treatment not always supported by the patients [32].

Despite this, various investigations on these treatments are still being conducted to overcome the obstacles they imply. One of the treatments studied today portrays the hyperthermia therapy, which will be explored and discussed in the following section [33].

2.1.1 Hyperthermia Therapy and Nanotechnology Advancements

For a long time, the ability of heat creation to heal has been widely understood and employed in the treatment of numerous diseases [34]. As previously stated, hyperthermia procedure is based on the notion of subjecting body tissue to high temperatures, in order to harm and kill cancer cells (by apoptosis) or to render cancer cells more susceptible to the effects of radiation and specific anticancer drugs [35].

Different approaches have been used to apply hyperthermia in tumor regions such as radiofrequency, microwave, water-filtered infra-red-A, ultrasound and capacitive heating techniques, depending on the tumor location, but with harmful secondary effects in the healthy tissues [4]. Although this therapy can increase the intracellular temperature up to the cellular death, one of the main limitations is that both cancerous and non-cancerous cells are in general equally sensitive to heat. Therefore, one of the most challenging aspects of hyperthermia is to keep a sufficiently high temperature on the tumour, while keeping the normal tissues at a lower temperature, so that normal cells aren't damaged [36].

This encouraged the research and development of new strategies capable of increasing the temperature of damaged areas, while keeping the rest of tissues healthy. Nanotechnology has been

brought into biomedical applications in the hopes of changing present diagnostic and treatment approaches with the use of NPs [4][37][38].

NPs can absorb energy from an external source and so improve the effects of hyperthermia. In reality, NPs serve as the principal heat source and reverse the direction of heat loss, using direct energy from an external source onto the tumor, causing localized thermal death while reducing the impact in collateral tissues. Based on this, nanotechnology advancements have recently permitted, by the use of magnetic NPs (MNPs), the application of a localized hyperthermia therapy [39]. This magnetic hyperthermia allows to remotely induce local therapy due to the capacity of certain MNPs to convert electromagnetic radiation into heat, which could rise the temperature in well-defined locations of the human body containing tumor cells [40][41].

2.1.1.1 Ferromagnetic NPs and Applications

MNPs have a huge potential in biomedical applications for controlled drug release [42]–[44], hyperthermia [45], magnetic resonance imaging diagnosis (MRI) [46][47], gene therapy and regenerative medicine [48] (Figure 1).

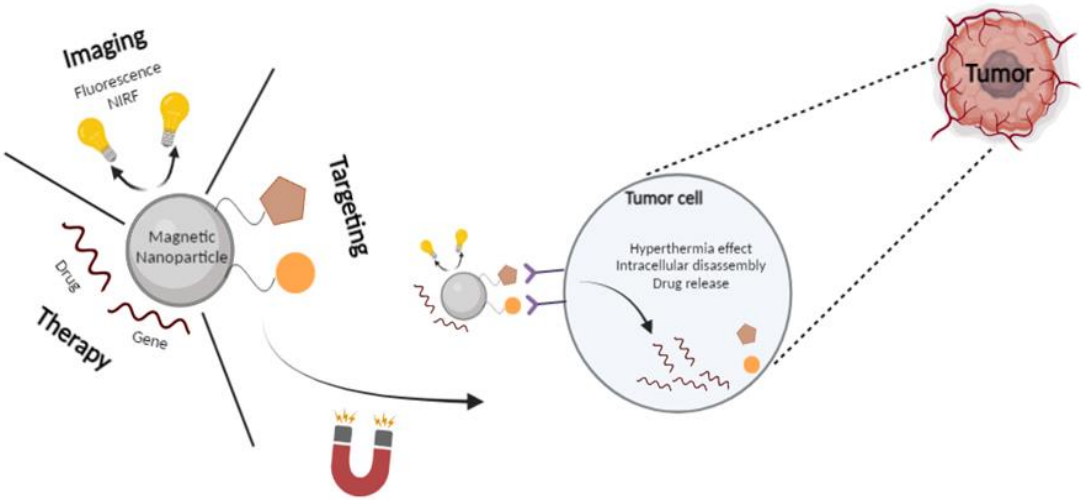

Figure 1: Illustration of MNPs applicability [43].

These NPs are typically classified into pure metals, metal oxides, and magnetic nanocomposites. The most popular MNPs in the biomedical field are Cobalt (Co), Iron (Fe), Nickel (Ni), Titanium (Ti), Iron Oxide and some ferrites [49].

Although this, the most often utilized materials for magnetic hyperthermia are nanometer-sized ferrite NPs, specifically magnetite (Fe_3O_4) once these nanoparticles are non-toxic and exhibit interesting magnetic properties resulting from its structure, due to the presence of iron cations in two valence states in a reverse spinel structure. In fact, the magnetic behavior of these NPs results from the cations (Fe^{2+}) since these ions reside only in octahedral zones, unlike Fe^{3+} ions that are equally distributed between octahedral and tetrahedral positions [50].

For these reasons, several types of magnetite nanoparticles have been developed and studied for intracellular hyperthermia with different magnetite core sizes [51]. This aspect is also relevant because, in general, magnetic characteristics also depend on particle size and on the preparation, methods used to produce the MNPs. As the nanoparticle size decreases, multi-domain ferromagnetic characteristics change to single-domain ferromagnetic, and finally, to superparamagnetic characteristics [52].

In an article by Atsumi *et al.,* magnetic NPs suitable for hyperthermia were discussed in terms of their magnetic properties, practical limitations in treatment conditions, and of the instruments used to activate the magnetic particles. By considering the magnetic and biocompatibility of the particles, superparamagnetic magnetite was considered the most promising [53]. These NPs, within the size range of less than 10 nm, can behave magnetically only under the influence of an external magnetic field and are rendered inactive once removed behave due to the presence of the state already mentioned and called superparamagnetism. This behavior of superparamagnetic materials results in potential advantages for delivering therapeutics onto specific sites or serve as heater for magnetic hyperthermia under the influence of an external magnetic field. According to Zhao *et al.,* these NPs modify the alternating magnetic field energy into heat by physical mechanisms (agitation of the magnetic nanoparticles due to the presence of the oscillating magnetic field) and the effectiveness of this transformation strongly depends on the frequency of the external field and the essence of the particles. The heating varies depending again on the size of the particles and it is created by hysteresis loss or relaxational loss [54].

In short, these NPs present several advantages already mentioned when compared to other metal NPs like Cobalt, Nickel, and Titanium due to their biocompatibility and stability, as well as biodegradability, ease of surface modification, functionalization and the state of superparamagnetism [55][56]. Putting it all together, these NPs show the ability to serve biomedical applications on the area of hyperthermia, but that doesn't end here.

In addition to hyperthermia, these MIONs (Magnetic Iron Oxide Nanoparticles) can be used as a contrast agent in computed tomography and MRI at low doses, with numerous MIONs previously approved by the Food and Drug Administration (FDA) for these uses. This is especially important since the concentration of MIONs within the tumor may be determined using computed tomography, which can help with hyperthermia dosimetry estimation [57]. They also show the possibility to bind to a variety of drugs, proteins, enzymes, antibodies or other molecular targets that makes them even more prominent and interesting in applications like systems for drug targeting [56].

In order to prove this, Table 2 shows different research works reporting the potential of MIONs with their respective applicability and results in biomedical field.

Table 2: Application of ferromagnetic NPs in different biomedical fields

NPs composition	Purpose	Description and Results
(Fe_3O_4)–(y- Fe_2O_3)	Hyperthermia	Structural and magnetic characterization of MIONs of variable sizes and narrow size variances. The NPs were prepared by a surfactant-assisted thermal decomposition approach in organic solvents based on a seeded-growth technique. All samples had narrow size ranges and demonstrated great stability in both organic and aqueous conditions without the presence of aggregates, making them suitable candidates for hyperthermia research [45].
Fe_3O_4 mannose/ribose/rhamnose	Hyperthermia	Synthesis and characterization of water dispersible sugar-coated iron oxide NPs designed as magnetic fluid hyperthermia heat mediators and negative contrast agents for magnetic resonance imaging. The influence of an inorganic core size was also investigated. MIONs were prepared by

		thermal decomposition of molecular precursors and then coated with organic ligands. The results showed that these synthesized nanoobjects could be fully dispersed in water, forming colloids that were stable over very long periods of time, and that iron oxide NPs of 16-18 nm were found to represent an efficient bifunctional targeting system for theragnostic applications, as they had very good transverse relaxivity and large heat release when radio frequency electromagnetic radiation with amplitude and frequency close to the human tolerance limit applied [58].
(Fe_3O_4)–(Au)	Hyperthermia	Study of the influence of a gold nanoshell on superparamagnetic iron oxide NPs for hyperthermia treatment and details on the importance of frequencies of oscillating magnetic field, concentration, and solvent on heat generation. Results showed that with or without the gold coating, when a low frequency oscillating magnetic field is applied, both MNPs emit heat. It was also shown that in the absence of oscillating magnetic field, both MNPs weren't particularly cytotoxic to mammalian cells [59].

Fe_3O_4	Hyperthermia	Coprecipitation of Fe^{3+} and Fe^{2+} with aqueous sodium hydroxide (NaOH) solution resulted in MNPs with varying magnetic characteristics. For local hyperthermia, the inductive heat characteristics of NPs in an alternating current (AC) magnetic field were examined. After 29 minutes in an alternating current magnetic field, the temperatures of a physiological saline solution containing Fe_3O_4 NPs ranged from 42 to 97.5 °C, indicating a potential application for hyperthermia treatment [60].
(Fe)–(Fe_3O_4) phosphatidylcholine	Hyperthermia, MRI	Study of the synthesis and surface engineering of core/shell-type iron/iron oxide NPs synthesized from microemulsions of NaBH4 and $FeCl_3$, followed by surface modification in which a thin hydrophobic hexamethyldisilazane layer is added. Comparison between iron oxide NPs and composite NPs. The resultant nanocomposite particles had a biocompatible surface and demonstrated excellent stability in both air and aqueous solution. The nanocomposites performed better in an alternating magnetic field than iron oxide NPs [61].
Fe_3O_4 oleic acid	MRI	Thermal degradation of Fe(III) glucuronate produced monodisperse Fe_3O_4 NPs coated with oleic acid. To make the Fe_3O_4 NPs dispersible in water, the particle surface was modified

		with α-carboxyl-ω-bis(ethane-2,1-diyl)phosphonic acid terminated-poly(3-O-methacryloyl-α-D-glucopyranose). NPs were evaluated on rat mesenchymal stem cells to investigate particle toxicity and cell labelling capabilities. The results revealed that the tagged cells still generated obvious contrast enhancement in the magnetic resonance image and that the NPs had no effect on cell survival [62].
Fe_3O_4 citrate DOX	Drug targeting	Demonstration on the approach for the fabrication of citric acid functionalized (citrate-stabilized) Fe_3O_4 aqueous colloidal magnetic NPs using soft chemical route and study the drug-loading efficiency of these using doxorubicin (DOX) hydrochloride. Results showed good stability, optimal magnetization, good specific absorption rate (under external alternated magnetic field) and cytocompatibility with cells [63].
Fe_3O_4	Drug targeting	Synthesis, antibacterial and heat evaluation of MIONs made in the presence of three carboxylic acid functionalized organic ligands (tiopronin, oxamic acid and succinic acid) using a co-precipitation method. The samples prepared with tiopronin and succinic acid were close to neutral pH and were suitable for magnetic fluid hyperthermia testing on *Staphyloccocus aureus* [64].

As stated before, the type of synthesis of MIONs is really important to the magnetic characteristics of the NPs. Various techniques of synthesis of MIONs have also been utilized to reach the aim of hyperthermia just like mentioned in Table 2, but the most prevalent are chemical precipitation, microemulsion, hydrothermal synthesis, and thermal breakdown.

In fact, one of the most studied syntheses for magnetite is the coprecipitation process [65]. Coprecipitation synthesis involves aqueous solutions of iron salts in several oxidation states (Fe^{2+} and Fe^{3+}) and subsequent precipitation with hydroxide. It is a quick and easy process that yields particles ranging in size from 5 to 180 nm. Coprecipitation has various benefits, including low reaction temperatures, short reaction times, cheap cost, chemical homogeneity, obtention of particles at nanoscale, products with high reactivity and uniformity, low agglomeration and the ability to process on a wide scale [66]. The final pH of the precipitation solution, ionic strength of the medium, concentration and molar ratio of the ions, precipitation temperatures, and stirring speed are among the parameters that determine the nature and features of the particles (homogeneity, size, magnetic behavior) [66]. Therefore, this will be the process used to produce the MNPs in this study.

However, despite the advantages of having better chemical stability and biocompatibility, there are major drawbacks on using NPs by themselves. One of them is the significant amount of NPs that is necessary to ensure constant tumor absorption. Another issue is that these NPs may not reach the intended target location which is critical in this sort of application once certain tissues are really deep and finally, because of their hydrophobic surfaces and the large surface area to volume, in the in vivo use of MNPs, they tend to agglomerate and to be rapidly released by the circulation. Therefore, the incorporation of these NPs onto drug delivery systems like polymeric fibrous structures, emerges as a solution to overcome most of the disadvantages described above [66][20].

2.1.2 Localized Drug Delivery Systems

Traditionally, drugs are delivered systemically into the body via the oral or intravenous routes. The therapeutic concentration of a drug is maintained in the body through repeated drug administration in both of these modes of administration. However, the systemic concentration of medication in the body peaks and falls fast during each repeated administration, especially when the drug's clearance rate is quite high. This can result in a seesaw effect in which the drug concentration in the body is either too low to give therapeutic benefit or too high, potentially leading to undesirable side effects. Non-target site toxicities are also related with systemic drug administration, which is a severe problem,

particularly with anticancer and new biotechnological treatments. Another downside is the patient's low compliance with repeated drug delivery [67].

By the use of localized drug delivery systems some of the described drawbacks may be overcome. Drug delivery systems are designed to provide the delivery of therapeutic drugs in a targeted and/or regulated manner. These systems evolved into a viable and practical technique of resolving many of the challenges associated with traditional pharmaceutic compound delivery. The optimal drug delivery system should be biocompatible, inert, mechanically strong, capable of high drug loading and safe from inadvertent release. The benefit of such a system is that the therapeutic concentration of a drug can be maintained in the body for longer periods of time without recurrent administration, boosting patient compliance, reducing drug under/overdosage concerns and delivering it to the specifically required location [67].

Current localized drug delivery systems are in the form of drug-eluting films, hydrogels, fibrous structures, wafers, rods, microspheres between others [68]–[71].

In this work, the drug delivery systems used will be fibrous structures. Numerous studies have already been done in order to be able to conclude on the potential of this whole procedure [71], [72], [81], [82], [73]–[80].

2.2 Fibrous Structures as localized drug delivery systems

Fibrous structures are very promising materials to be used as localized drug delivery systems for cancer treatment and so they have emerged as an appealing option. The main justifications for the growth of this approach are based on the fact that they present ease on their fabrication, generally high mechanical properties, desirable drug release profile and high surface area to volume ratio [71].

In regard to their processing, these structures could be based on biodegradable polymers with also low immunogenicity, meaning that, with the application of these structures, there won't be strong immune responses from the patient's immune system. Additionally, these structures can be adjusted by changing the polymers used to make them, as well as their length and cross-sectional radius, to find the best composition and morphology for the application required [71].

For all these reasons, a combination of fibrous structures and NPs has the potential to maximise the effective functional output from NPs in the desired target, which will result in the enhancement of cancer therapy efficiency and the reduction of side effects, improving the patient's life quality [83][84][85].

2.2.1 Fibrous Structures with Ferromagnetic NPs

As stated before, fibres containing magnetic NPs reveal a huge potential for many applications, that could be: magnetic filters, sensors, magnetic shielding devices and magnetic induction devices and even protective multifunctional systems [86][20]. For this very reason, some studies have been developed in order to comprehend the behaviour of this systems with NPs.

Wang *et al.,* reported the production and characterization of superparamagnetic composite polymer/magnetite nanofibres, searching for their mechanical properties and behavior. As it is stated, using magnetite nanoparticle suspensions in PEO and PVA, they obtained polymer nanofibres ranging in diameter from 140 to 400 nm and verified that both sets of fibres responded to an externally-applied magnetic field by deflecting in the direction of increasing field gradient, showing also that magnetite NPs reinforced the mechanical properties of the nanofibres, as expected [87].

In another study, made by Miyauchi *et al.,* polyvinylpyrrolidone fibres with high concentrations of ferromagnetic and superparamagnetic NPs were also developed and the magnetic properties of these

fibres were then explored, using a superconducting quantum interference device. They concluded that mixed magnetic composites may offer an important platform for better understanding the magnetic properties of materials and provide a scalable process for the fabrication of nanocomposites with novel magnetic properties [88].

Nevertheless, it is important to mention some articles where the use of this combination is verified for the desired application: cancer treatment.

Thus, in a study made by Kim *et al.*, a magnetic composite nanofibre mesh that could achieve mutual synergy of hyperthermia, chemotherapy, and thermo-molecularly targeted therapy for highly potent therapeutic effects was produced. The nanofibre was composed of biodegradable poly(ε-caprolactone) with DOX, magnetic NPs and 17-allylamino-17-demethoxygeldanamycin. The developed nanofibres mesh exhibited hyperthermia, good biocompatibility, a sustained and pH-sensitive release behavior that was favorable for the long-term maintenance of effective drug concentration in tumor tissue. In MCF-7 cells (a breast cancer cell line), this nanofibre mesh efficiently induced apoptosis, reveling its potential as a new tumor therapy and as an effective locally implantable system for enhancing the efficacy of combination cancer treatments [89].

In another study, by Tiwari *et al.,* it was developed a magnetically actuated smart textured fibrous system based on polycaprolactone with MIONs, anti-cancer drug (DOX) and fluorescent carbogenic nanodots. This system demonstrated enhanced heating with the application of an alternating magnetic field that led to an increase in drug release and enhanced the efficacy of the therapy, also showing the ability to navigate in the fluid with the application of gradient magnetic field. Further, this system was nontoxic to cells and do not leach out any toxic material to them during incubation, proving that it is a potential candidate in the field of cancer therapy [90].

Sasikala *et al.,* also reported on this subject, a smart nanoplatform responsive to a magnetic field to administer both hyperthermia and pH-dependent anticancer drug release for cancer treatment. To achieve this, MIONs were incorporated onto the nanofibres matrix. These nanofibres were developed by electrospinning (ES) with a biocompatible polymer, poly(D,L-lactide-co-glycolide). In regard to the anticancer drug delivery, this step was performed by surface functionalization using dopamine to conjugate the bortezomib through a catechol metal binding in a pH-sensitive manner. The *in vitro* studies confirmed that this device exhibited a synergistic anticancer efficacy due to the simultaneous application of hyperthermia and drug delivery, providing a secure pathway for delivering the anticancer drug specifically towards the tumor, as well as the retention of the magnetic NPs in the tumor region in a sufficient concentration for hyperthermia treatment [91].

Kim *et al.*, reported another example of smart hyperthermia nanofibres with simultaneous heat generation and drug release in response to 'on-off' switching of alternating magnetic field. The nanofibres were composed of a chemically-crosslinkable temperature-responsive polymer (Poly(NIPAAm-co-HMAAm) with an anticancer drug (DOX) and MNPs. In the results shown, 70 % of human melanoma cells died in after only 5 minutes of alternating magnetic field application in the presence of this device, by double effects of heat and drug, showing again the immense potential on this area [92].

Finally, Lin *et al.,* used Fe_3O_4 NPs incorporated onto crosslinked electrospun CH nanofibres using chemical coprecipitation. Such system could be delivered to the treatment site precisely by surgical or endoscopic method. They also grafted iminodiacetic acid onto the CH with an aim to increase the amount of magnetic NPs formed in the magnetic nanofibre composite. The results of this study revealed that this incorporation led to more magnetic NPs formed in the matrix of the nanofibre. In addition, the magnetic iminodiacetic acid-grafted CH nanofibre composite showed that could reduce the proliferation/growth rate of malignant cells of the tumor under the application of magnetic field [93].

Based on the good results obtained in the previously mentioned papers using fibrous structures as drug delivery systems, it was necessary to choose the method of processing them for this work. Therefore, in order to do so, it's important to understand that over the past few decades, various methods have been used for the fabrication of micro and nanofibres. WS, rotary spinning, ES, microfluidic fibre fabrication, and self-assembly are the most common methods [71]. However, in this thesis, the main focus will be WS once this process offers the advantage of producing a wide variety of fibre cross-sectional shapes and sizes and the possibility to work at lower temperatures, while also allowing to use different polymers and not being too expensive. Hence, it's important to fully understand the concept behind this technique and some of the most used polymers [94].

2.3 WETSPINNING - TECHNOLOGY AND PROCESS OPERATION

WS consists in a non-solvent induced phase inversion that enables the creation of polymeric microfibres with a homogeneous shape using the precipitation concept. In fact, in many studies developed with this technique, various medicinal agents such as chemotherapeutics [82][76], antibiotics [95][96] and nonsteroidal anti-inflammatory medications [97][98] have been loaded into these fibrous structures, showing the possibilities opened by it. Generally, a WS equipment consists of four key components: the first is a syringe pump or a gravitational pull that will be responsible for pumping the polymeric solution, which is the second component, in the third component, that is the coagulation bath. Sometimes WS set-up also comprises a spinneret [94].

So, in general, the solution is extruded directly into the coagulation bath and solidifies upon contact with the non-solvent throughout the spinning process, creating the fibres. The shape and diameter of these fibres is affected by thermodynamic conditions of the polymeric solution and the coagulation bath and also by factors like the viscosity of the polymeric solution, the injection rate and the size of the spinneret [71].

Aside from the ability to control the diameter of the resulting structures, fibres produced by WS typically have large pore sizes, resulting in beneficial improvements in cell adhesion and penetration within scaffolds and films. Another advantage is the possibility to create fibres with low processing temperature [99].

2.3.1 OPERATING PARAMETERS

A collection of processing factors that can influence the morphology, shape, diameter, and mechanical performance of the produced fibres has a considerable impact on the WS process. This collection of parameters is organized into three major groups in Table 3, which comprise solution, process, and environmental factors:

Table 3: Operating parameters of WS

Process Parameters	Solution Parameters	Environmental factors
Coagulation Bath	Polymers molecular weight	Humidity
Coagulation Bath Temperature	Polymers concentration	Drying temperature
Flow Rate	Viscosity	
Needle Diameter	Solvent	

2.3.2 Fibrous systems based on Chitosan, PEO and PVA

Typically, synthetic and natural polymers are blended to increase the performance of the created biomaterial, overcoming the limits of each polymer when employed alone. For the production of fibres by WS, many different polymers have been studied, as well as mixtures of polymers, always based on the final objective and the characteristics needed. Therefore, in this part of the study, the polymers chosen will be addressed in order to understand their usefulness and importance [100].

2.3.2.1 CH

CH is a copolymer made up of multiple monomeric units of glucosamine and N-acetyl-D glucosamine with β(1→4) bonding (Figure 2) and its solubility is proportional to the number of protonated amine groups in the polymer chain. When CH is dissolved in acid, the amino groups in the chain protonate and the polymer becomes cationic, allowing it to interact with a wide range of molecules. This positive charge is assumed to be responsible for its antibacterial function since it interacts with microbes' negatively charged cell membranes [101].

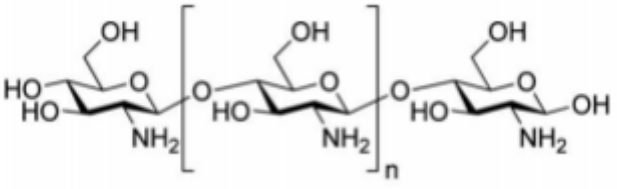

Figure 2: Chemical structure of CH [78].

Because CH is soluble in acidic environments, acids must be used [102][103]. CH conjugates can be generated depending on the acid used, resulting in the production of a complex that combines the characteristics of CH and the acid utilized.

Because of its solubility in weak acid solutions, chitosan may be synthesized into multiple forms under considerably gentler conditions than its parent polymer chitin, making chitosan a more appealing biopolymer for a number of applications. For this and for the fact that CH is biocompatible, biodegradable, nontoxic and has wound healing and antibacterial capabilities, this polymer is receiving a lot of attention in the pharmaceutical and biomedical industries, which leads to the continuing study of this polymer for a wide range of biological applications [104].

East and Qin reported the first application of chitosan in WS in 1993. They concluded that chitosan fibres could be created by the wetspinning of its solution in dilute aqueous acetic acid and that the fibres properties were affected by the spinning conditions, such as spin stretch ratio, coagulation bath concentration and drying conditions [105].

In another article written by Shigerino Hitano *et al.*, a study of chitin and chitosan fibres obtained through WS was conducted, where the characteristics required for their applicability in different areas such as textiles, industrial materials, and medical and biotechnological materials was verified [106].

In other study made by School of Biological Sciences, it was demonstrated that drug-loaded hydrogel fibres made with CH could be used as a device capable of delivering sustained high concentrations of gemcitabine locally, achieving tumor control, with minimal toxicity for localized therapy of pancreatic cancer. This device was also produced by WS [82].

Vega *et al.*, also prepared and studied the properties of CH–PVA fibres produced by WS. In this article, they studied and analyzed different properties such as the polymers concentration, the coagulation bath and the crosslinking solution. Finally, they concluded that they could create fibres with mechanical characteristics and morphologies that are acceptable for a variety of specific applications [107].

As can be seen CH nanofibres have a high potential for biomedical applications, however sometimes their characteristics are not in the ideal values, showing limited water resistance, and a poor capacity to absorb bodily fluids. For hence, combining CH with other polymers, such as PEO or PVA, and using a crosslinking agent are common techniques for improving some of these properties.

CH Crosslinking

The mechanical integrity of natural polymers, specifically chitosan, must be improved before implantation into the body [108][109]. For this reason, crosslinking fibres would be a viable option.

To reinforce the chitosan nanofibrous structure in solid/aqueous environments, various crosslinking methods have been used. Physical crosslinking is one of the two types of crosslinking that has been used the most for chitosan. This type of crosslinking results from the dehydration of the chitosan acetate salt via amide bond formation [110]. In the other hand, the other crosslinking used is chemical crosslinking, that results from covalent bonds formed between the amino (–NH2) or hydroxyl groups (–OH) of chitosan with the chemical of interest [111][112].

As said, these crosslinking strategies may improve mechanical strength of the fibres and conduction in conductive material that will be essential in their development, as well as drying, which will also contribute to these properties [109].

To produce a crosslinking there must be one or more crosslinking agents. These crosslinkers are molecules that contain two or more reactive ends capable or chemically attaching to specific functional groups (primary amines, sulfhydryl's, etc.) on proteins or other molecules [113].

In this case, since the work is directed to develop a structure based on chitosan it is important understand what agents can crosslink this polymer and what work has been done in this field, giving special attention to the chemical crosslinking, once it's the one being used in this thesis.

Hence, in the following Table 4 are some types of crosslinking done in some articles.

Table 4: Crosslinking systems applied on fibres

Fibres produced	Crosslinking system	Reference
Chitosan/poly(ethylene oxide) nanofibres	Glutaraldehyde (GTA)	[114]
Chitosan Fibres	Sodium triphosphate (TPP)	[113]
Chitosan/poly(ethylene oxide) nanofibres	GTA	[109]
Chitosan Fibres	Epichlorohydrin	[115]
Chitosan-PVA Fibres	GTA/TPP	[105]

Based on this table, three crosslinkers have especial attention in the articles where fibres from CS are produced. Knowing by literature that epichlorohydrin has been reported as toxic to cells sometimes, in this thesis the other two options will be explored [115]. As mentioned earlier, in addition to crosslinking, the conjugation of polymers such as PEO and PVA could also improve the properties of CH.

2.3.2.2 PEO

Poly(Ethylene Oxide) is an extremely biocompatible and biodegradable polymer, since it has the capacity to interact with polarized surfaces and is often inexpensive, making it an appealing biomaterial. In addition, it is hydrophilic, linear and readily soluble in both aqueous and organic solvents [116][117].

The repetitive structural unit of polyethylene oxide, PEO, is shown on Figure 3.

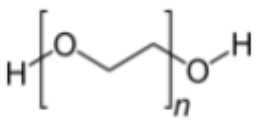

Figure 3: Chemical structure of PEO [87].

PEO may be used with CH and other polymers to improve mechanical properties and the spinning process. This polymer has been studied in many different areas, not excluding the one that is it most important for this thesis: the production of fibres. However, there are not many articles that reported the use of these two polymers for the production of wet-spun fibres, reinforcing the innovative character of this work. Still, some conclusions can be draw about the use of these polymers together from articles that reported the use of another technique (ES).

As a matter of fact, in a study made by Fatemeh Kalalinia *et al.*, the authors focused on developing a new effective topical drug delivery system. Nanofibres of CH/PEO containing vancomycin (VCM) were successfully fabricated. The results showed that the CH/PEO/VCM fibres had very good mechanical, biomechanical, antimicrobial properties and an effective healing effect [114].

Also, S. Abib *et al.* created CH/PEO nanofibres with high antibacterial capabilities, good thermal stability, regulated antibacterial agent release and no toxicity in cutaneous and keratin fibroblast cell lines, allowing them to be used in the prevention and treatment of wounds and burns [118].

In another one, Guiping Ma *et al.* made the characterization of CH/hyaluronic acid nanofibres. In this article, they obtained a highly porous CH nanofibres membrane by using CH/PEO and then removing PEO with water. Then, the porous nanofibres were soaked in 0.1 wt % paclitaxel solution to load the cancer drug and a polyanion nature macromolecular hyaluronic acid was encapsulated on the chitosan polycation porous nanofibres. The nanofibres' activities in vitro on DU145 prostate cancer cells were investigated and cell culture findings revealed that the nanofibres mats were effective in preventing cell attachment and growth [119].

Finally, Jafari A *et al.* conducted a study in order to recognize CH/PEO/Berberine (BBR) nanofibres effect on cancer cell lines. An inverted microscope was used to examine the development and proliferation of human breast cancer cell lines, human HeLa cervical cancer cells, and fibroblast cells in cultured media. When compared to the control group cell lines, nanofibres containing 0.5-20 wt % BBR concentrations reduced cell proliferation. Cancer cell lines' viability was drastically reduced after being exposed to CH/PEO/BBR [120].

2.3.2.3 PVA

Poly(vinyl alcohol) (PVA) (Figure 4) is a polymer that has been studied intensively because of its good film forming and physical properties, high hydrophilicity, processability, biocompatibility, and good chemical resistance [12][13].

Due to the instability of vinyl monomer, unlike other polymers, PVA cannot polymerize from its own monomer and must instead use poly(vinyl acetate) (PVAc). As a result, PVA can only be made from PVAc by saponification or alcoholysis (reacting PVAc with methanol). PVAc can be hydrolyzed into two grades: fully hydrolyzed and partly hydrolyzed, depending on the application. The degree of hydrolysis reflects the amount of remaining acetate groups in the polymer that have not undergone saponification or alcoholysis. The degree of hydrolysis will eventually affect the properties of PVA including its solubility [121].

PVA/natural fibre composites have limitless application possibilities in a variety of sectors, especially as the focus shifts away from synthetic materials and toward biodegradable materials. Because of their ecologically beneficial and user-friendly properties, this phenomenon has provided a plethora of prospects for such materials.

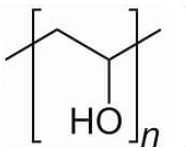

Figure 4: Chemical structure of PVA [122].

For example, in an article by Yan *et al.,* PVA/CS nanofibres were successfully fabricated. With the change of the feed ratio between PVA and CS, the surface morphology and the microstructures of the nanofibres were largely changed. These fibres were used as a carrier for DOX delivery onto human ovary cancer cells. The results of in vitro cytotoxicity test indicated that fibres were biocompatible and showed less cytotoxicity than the free DOX. Via observing by confocal laser scanning microscopy, it was possible to confirm that the prepared fibres exhibited controlled release of DOX into the cancer cell nucleus, which were effective in prohibiting the ovary cancer cells attachment and proliferation, a step very important for the tumor therapy [123].

In another article by Yan *et al.,* polycaprolactone/polyvinyl alcohol (PCL/PVA) nanofibres with pH-responsive properties were also successfully prepared and could be used as carriers for an

anticancer drug called paclitaxel. These paclitaxel loaded fibres showed pH-responsive release of the drug and after cultured with colon cancer cells showed that they can inhibit the proliferation and growth of the cells completely, even killing them, showing once more the promising abilities to be used as biomaterials in cancer therapy of some tumors [124].

To prove once more the use of this polymer in cancer area, Qavamnia *et al.*, loaded DOX-hydroxyapatite into the CH/PVA/Polyurethane nanofibres. The potential of synthesized nanofibres was evaluated for controlled release of DOX-hydroxyapatite and bone cancer treatment in vitro.

The DOX-hydroxyapatite encapsulation efficiency on fibres was higher than 90 % and its sustained release was obtained within 10 days under acidic and physiological pH. The cell attachment and cell death results also indicated the great potential of these loaded fibres for bone cancer treatment [125].

In conclusion, as it can be seen from the review of all these articles, the polymers mentioned here can be used to produce fibrous structures capable of acting as drug delivery systems for the treatment of various cancers. By conjugating these structures with MNPs, the possibility of using hyperthermia for cancer treatment will be raised.

3 Materials and Methods

In this work, three polymeric formulations were optimized to produce fibres by WS: CH, CH/PEO and CH/PVA. Each of these was tuned at both the solution and process levels, including the percentage of polymer(s) in solution and type of solvent, as well as the needle diameter, flow rate, and coagulation bath.

The next part summarizes the optimum parameters of the solutions acquired this far, which enabled the production of fibres and the processes employed for the various polymer solutions. In addition, the methodologies for fibre characterization are discussed.

3.1 MATERIALS

For the development and optimization of the various polymeric formulations, three biodegradable polymers PEO, CH, PVA and NaOH as a coagulation bath were used. It was also used acetic acid, in order to help in the dissolution of CH. Table 5 shows the materials used.

Table 5: Characteristics of the materials used in the development of various polymeric systems

Polymers	**Supplier**
CH (high molecular weight 100,000-300,000)	Sigma Aldrich
PEO (Mv 900,000)	
PVA (Mv 146,000-186,000)	
Acid	
AcOH glacial 99-100%	Chem-lab
Coagulation Bath	
NaOH, pellets	Normax
Crosslinking Bath	
TPP	Scharlau

Wetspinning system

The WS process was performed in an equipment illustrated in Figure 5, with a pump from the brand New Era Pump Systems Inc..

Similar to the others WS equipments and as previously mentioned, the equipment used in this study is composed of a place to put the syringe, a pump capable of extracting the polymer solution to be tested and a compartment where the bath is placed.

The polymer solution to be tested was placed in a 24 mL syringe, and different needle diameters (Ø 0.61 mm and Ø 0.41 mm) were used. To remove the fibres from the bath, tweezers and pipettes were used.

Figure 5: WS equipment.

3.1 METHODS

3.1.1 FORMULATIONS OF CHITOSAN

Preparation of the solution

The CH solution was optimized by testing different concentrations, 2 %, 3 % and 4 %. For the dissolution of the CH, as mentioned before, acetic acid was used. Different concentrations were tested: 2 %, 6 %, 12 % and 50 %, to ensure the correct dissolution of CH. The experimental procedure for the production of the CH fibres by WS is summarized in Figure 6.

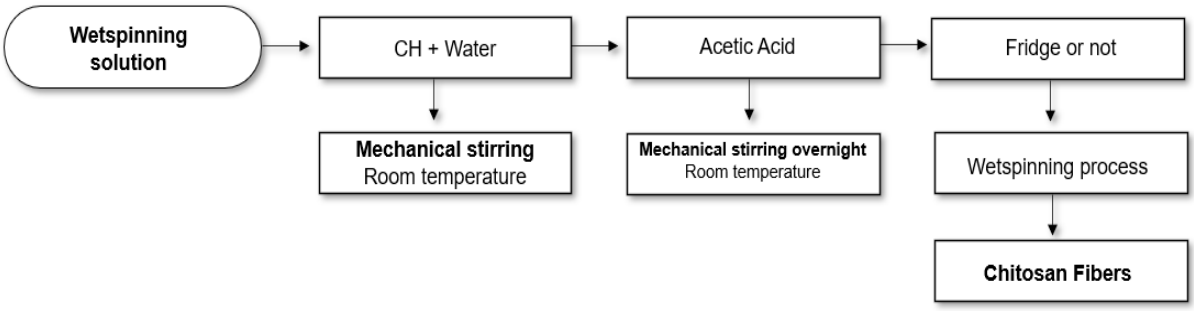

Figure 6: Procedure executed to obtain CH fibres.

Initially, the CH was added in the desired concentration (after sieving) to the water and left to stir continuously until dissolved. Then the corresponding acetic acid was added slowly, and the solution was stirred until the next day. After this, the solutions were centrifuged for 20 minutes at 4000 rpm. Some solutions were placed in the fridge and others were not, so that two different temperatures could be tested.

WS Parameters

After having the desired solutions, they were transferred to syringes and WS tests were performed with two different needle diameters - Ø 0.61 mm and Ø 0.41 mm - and three different baths, also varying the flow rate. A summary of the parameters that were used, both in relation to the WS parameters and to the concentrations of the solutions is described in the following Table 6.

Table 6: Parameters changed to obtain different CH fibres

Solution	Bath	Conditions
2 % CH with 50/50 water and AcOH	1 M NaOH	Room temperature, 0.41 and 0.61 mm needles
	2 M NaOH	Room temperature, 0.41 and 0.61 mm needles
2 % CH with 2 % AcOH aqueous solution	1 M NaOH	Room temperature or after fridge, 0.41 and 0.61 mm needles
2 % CH with 6 % AcOH aqueous solution	1 M NaOH	Room temperature or after fridge, 0.41 and 0.61 mm needles
	2 M NaOH	Room temperature or after fridge, 0.41 and 0.61 mm needles
3 % CH with 12 % AcOH aqueous solution	1 M NaOH	Room temperature or after fridge, 0.41 and 0.61 mm needles
	2 M NaOH	Room temperature or after fridge, 0.41 and 0.61 mm needles
4 % CH with 12 % AcOH aqueous solution	1 M NaOH	Room temperature or after fridge, 0.41 and 0.61 mm needles
	2 M NaOH	Room temperature or after fridge, 0.41 and 0.61 mm needles

3.1.1 CROSSLINKING

Crosslinking techniques were employed after WS. In order to do these, three different methods were tested to see in which of them resulted in the best fibers. Two of these methods were based on the steam deposition of the crosslinking agent and another one based on a bath of the same. In the first procedure tested, Figure 7A, the fibres were collected and placed on a net over a beaker containing different quantities of GTA in a dissector. After that, a part of the fibres was placed inside the oven at different temperatures and others at room temperature, to study the effect of different temperatures for 24 hours.

In the second procedure, the same idea was kept in mind but this time putting the fibres directly suspended in the beaker, leaving the net used before aside as shown in Figure 7B. Once again, GTA and different temperatures were used.

The last procedure consisted of a bath resulting from a solution with the selected crosslinking agent where the fibres were immersed (Figure 7C). In this procedure, two different crosslinking agents and mixtures of both were tested: GTA and TPP. Different temperatures of drying of the fibres after the bath were tested afterwards.

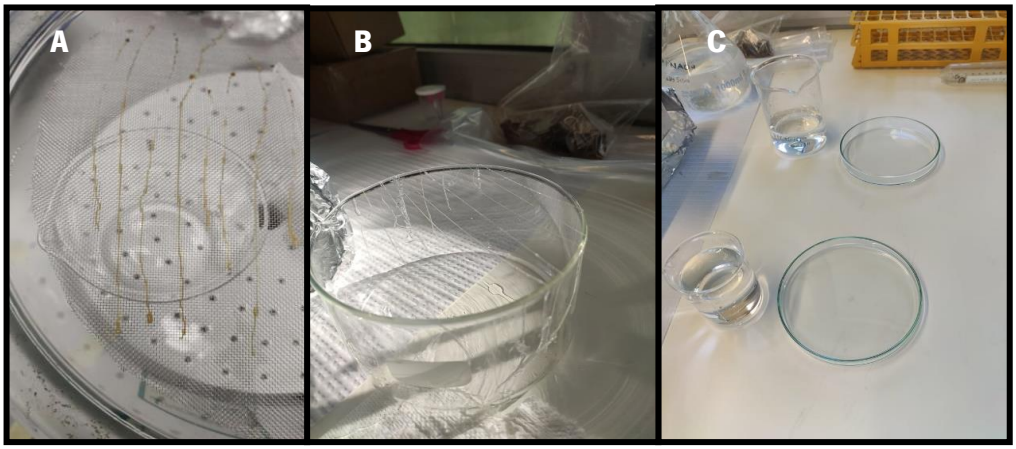

Figure 7: A) First procedure tested with fibres collected and placed on a net over a beaker; B) Second procedure with fibres directly suspending in the beaker; C) Third procedure with a bath where the fibres were immersed.

3.1.1 CHITOSAN/PEO FORMULATIONS

Preparation of the solution

After optimizing the solution of CH and AcOH, PEO was added in order to be able to benefit the mechanical properties and thermal stability of the fibres. Different PEO concentrations were then tested: 1 %, 2 % and 3 %. To prepare these solutions, CH (sieved) and PEO were dissolved in water under mechanical stirring, individually. After achieving the correct dissolution for both polymeric formulations, they were mixed and acetic acid was slowly added and left in stir overnight. The final solution was centrifuged at 4000 rpm for 20 minutes and was then placed in the fridge for further tests.

WS Parameters

After obtaining the final solution, the production of fibres by WS was performed using the needle with the best results so far (0.41 mm diameter), a flow rate of 1 mL/min. and a 1 M NaOH bath. In summary, the parameters used are shown in Table 7 below.

Table 7: Parameters used to obtain different CH/PEO fibres

CH + AcOH	PEO%	Bath	Conditions
3 % CH with 12 % AcOH aqueous solution	1 %	1 M NaOH	Temperature after being in the fridge and 0.41 mm needle
	2 %		
	3 %		

3.1.1 CHITOSAN/PVA FORMULATIONS

Preparation of the solution

A CH and PVA mixture was also tested. In this case, four different PVA concentrations — 2 %, 5 %, and 10 % — were evaluated. Both polymers were separately dissolved in water while being mechanically stirred to create these solutions. It should be noted that the PVA solution needed a temperature of around 30 °C to dissolve properly. After the proper dissolution of both polymeric formulations, they were mixture. The solution was stirred overnight while acetic acid was gradually added. The final solution was centrifuged at 4000 rpm for 20 minutes before being stored in the fridge.

WS Parameters

The synthesis of fibres by WS was carried out using again the parameters optimized from the last results: the needle with 0.41mm diameter, a flow rate of 1 mL/min and a bath of 1 M NaOH.

Table 8 below summarizes the parameters that were used.

Table 8: Parameters used to obtain different CH/PEO fibres

CH + AcOH	PVA%	Bath	Conditions
3 % CH with 12 % AcOH aqueous solution	1 %	1 M NaOH	Temperature after being in the fridge and 0.41 mm needle
	3 %		
	5 %		

3.1.1 Synthesis of Ferromagnetic NPs

For synthesizing the ferromagnetic NPs, a protocol previously described was adapted [126]. In the first step of the NPs production, two solutions were made: an acidic solution of Iron II Chloride (2 M) and an aqueous solution of Iron III Chloride (1 M). These solutions were subsequently mixed and an ammonium hydroxide solution (1 M) was added. The solution obtained was placed under stirring for 30 minutes.

After this, the solution was washed with water using a magnet attached to remove the material of interest. This material was subsequently dispersed in 250 mL of water, to which was added 2 mL of oleic acid and 5 mL of acetone. Again, the solution was placed under stirring for 30 minutes and the material of interest was separated using the magnet and washed with acetone. After this process, the leftover material was dispersed in 15 mL of cyclohexane and centrifuged for 30 minutes at 2000 rpm.

In order to obtain the NPs in solid state, the solution was placed in the oven at 150 °C for 3 hours. Following its synthesis, different percentages of synthesized NPs were added to the optimized solutions studied in order to reach the better results.

3.1.2 Development of the Fibrous Structures

For the production of the localized drug delivery structure composed by the optimized fibres produced by WS, three different approaches were tested. The first was the production by weaving: process of producing fabric by interlacing two sets of strands at right angles. The second was based on set the structure directly in the crosslinking bath, hoping that after it the fibres would dry and produce a well-structured form. The last procedure comprised in leaving the fibres in the crosslinking bath and after it making the structure by laying the fibres on themselves. In all of them, a Teflon sheet was used as platform to dry the structures.

3.2 Characterization Methods

3.2.1 Optical Microscopy

In the initial step, the optical microscope was utilized to analyze the arrangement and morphology of the produced fibres. This microscope employs visible light and an ocular lens system to create a magnified picture of the sample under examination, allowing the study of features that are not apparent to the human eye [106]. In this work, the fibres produced by the WS method were examined using a Leica DM750 M (bright field) Microscope equipped with two eyepieces and four objectives (5x, 10x, 20x and 40x).

3.2.2 Scanning Electron Microscopy (SEM)

SEM was also used to produce images of a sample by scanning the surface with a focused beam of electrons. The one used in this was NOVA Nano SEM 200, FEI Company (Hillsboro, OR, USA), instrument at 5000 and 50.000 × magnifications. All the fibres samples were added to aluminum pin stubs with an electrically conductive carbon adhesive tape (PELCO Tabs™).

3.2.3 Attenuated Total Reflectance - Fourier Transform Infrared Spectroscopy (ATR-FTIR)

The ATR-FTIR method was employed to investigate the interaction between the different polymers used and the chemical composition of the wetspun fibres produced. This method of vibrational spectroscopy vibrates the molecular bonds of the sample that absorbs infrared light and given that various samples have distinct molecular bonds or configurations, this approach may be used to learn the chemical makeup of the molecules found in each sample under study [109].

The chosen samples were subjected to an ATR-FTIR spectroscopic study using an IRAffinity-1S instrument from SHIMADZU (Kyoto, Japan) that has an ATR attachment. Each spectrum was recorded in a diamond ATR cell in transmittance mode using an accumulation of

45 scan cycles and an 8 cm^{-1} resolution. The machinery was set up to measure the samples' transmittance throughout a spectrum spanning 400 to 4000 $cm^{-1.}$

3.2.4 Scanning Transmission Electron Microscopy (STEM)

The Scanning Transmission Electron Microscopy (STEM) was used to study the morphology and size of the produced NPs. The microscope lenses are changed in scanning transmission electron microscopy mode to provide a focused convergent electron beam or probe at the sample surface. This focused probe is then traversed across the sample, collecting signals point by point to generate a two-dimensional picture.

The morphology of the synthetized NPs was studied using a NOVA 200 Nano SEM from FEI Company (Hillsboro, OR, USA) with a scanning transmitted electron microscopy detector.

3.2.5 Energy dispersive X-ray spectroscopy (EDS)

The samples were characterized using a desktop scanning electron microscope coupled with EDS analysis (Phenom ProX with EDS detector; Phenom-World BV, The Netherlands). All results for the quantification of the concentration of the elements present in the fibres were acquired using ProSuite software integrated with Phenom Element Identification software.

3.2.6 Thermogravimetric Analysis (TGA)

To confirm the thermal stability of the generated fibres, a TGA analysis was carried out [127]. In a STA 700 SCANSCI apparatus, the thermal behavior of the generated fibres was studied. The TGA curve was produced using nitrogen atmosphere, a temperature range of 30–600 °C, and a constant heating rate of 10 °C/min. The samples were put in a crucible that was attached to a microbalance for the analysis, and the mass loss was tracked while the crucible was gradually heated.

3.2.7 Mechanical Tests

The equipment used for these testing was a Hounsfield Tinius Olsen model H100KPS with a 250 N load cell. The samples were divided into strips that were 2.5 mm wide and 7.5 mm long. 50 mm was used as the first grasp separation value. The stress-strain curves were then used to compute the Young's modulus, elongation at break, and breaking point. Fibres and structures of fibres were analyzed.

3.2.8 Swelling Degree

The weight difference between the samples that were dry and those that were swelled was used to gauge the degree of swelling. For 24 hours, the dried fibres were submerged in water heated to 37 °C. The wet weight of the fibres was calculated after extra liquid was removed. Assuming that Ws is the mass of the swollen material and Wd is the original dry mass, the swelling degree was determined as follows and represented as a percentage of the dry sample:

$$swellingdegree\ (\%) = \left(\frac{Ws - Wd}{Wd}\right) x\ 100$$

3.2.9 *In Vitro* Degradation

The fibres were cultured in water for 24 hours at 37 °C. Following full drying in an oven set at 50 °C for 24 hours, they were weighed to determine the degree of degradation using the equation below, where Mi refers for initial dry mass and Mf represents for final dry mass:

$$weightloss\ (\%) = \left(\frac{Mi - Mf}{Mf}\right) x\ 100$$

4 Results and Discussion

As previously mentioned, the main purpose of this work is to develop polymeric formulations based on CH, PEO and PVA to produce microfibres by wetspinning. For this, several WS and solution parameters were optimized as could be seen in the following sections. After the optimization of the polymeric formulations, several fibres were produced and some of them were selected. In these selected formulations for the fibres production, NPs were added in different percentages to analyze their effect in the final fibres. After complete characterization and analysis of some properties, the best fibres were utilized to develop fibrous structures with possible application as localized drug delivery systems for magnetic hyperthermia.

4.1 Production and optimization of Chitosan Wetspun fibres

The first polymer tested for the production of fibres by wetspinning was chitosan. CH is a polymer that is widely utilized in the biomedical field and its solubility is related to the quantity of protonated amine groups in the polymer chain. When CH is dissolved in acid, the amino groups in the chain protonate, causing the polymer to become cationic and capable of interacting with a wide spectrum of molecules. AcOH was utilized in the preparation of the CH solutions for this purpose [128].

Several parameters, including pre-processing, percentage and proportion of the polymers, percentage of the solvent, needle diameter, temperature of the solution and post-processing of the solution mixture (centrifugation and homogenization), were evaluated and optimized to produce CH fibres. Also, three different baths were tested: 1 M NaOH, 2 M NaOH and 4 M NaOH. The 4 M NaOH was directly excluded once it was impossible to use, due to its adverse reaction with the material thanks to its high concentration. The formulations used are now described in Table 9.

Table 9: Optimizations of chitosan fibres

Solution	Bath	Conditions
2 % CH with 50/50 water and AcOH	1 M NaOH	Room temperature, 0.41 and 0.61 mm needles
	2 M NaOH	Room temperature, 0.41 and 0.61 mm needles
2 % CH with 2 % AcOH aqueous solution	1 M NaOH	Room temperature or after fridge, 0.41 and 0.61 mm needles
2 % CH with 6 % AcOH aqueous solution	1 M NaOH	Room temperature or after fridge, 0.41 and 0.61 mm needles
	2 M NaOH	Room temperature or after fridge, 0.41 and 0.61 mm needles
3 % CH with 12 % AcOH aqueous solution	1 M NaOH	Room temperature or after fridge, 0.41 and 0.61 mm needles
	2 M NaOH	Room temperature or after fridge, 0.41 and 0.61 mm needles
4 % CH with 12 % AcOH aqueous solution	1 M NaOH	Room temperature or after fridge, 0.41 and 0.61 mm needles
	2 M NaOH	Room temperature or after fridge, 0.41 and 0.61 mm needles

In the first formulation, when spun in the respective baths, the fibres appeared to form and in some sparse cases it was possible to extend it until the end of the bath, however they could not be removed because it gave rise to a gel-like structure that can be seen in Figure 8A. As the fibres weren't formed, it was understood that it was due to the excess of acetic acid. Thus, the concentration was reduced to 2 %.

Despite this and although the smaller needle diameter seemed to benefit the fibres (0.41 mm of diameter), the fibres produced in the second solution still showed many defects as can been seen in Figure 8B and 8C, something that could be due to the poor dissolution of the CH.

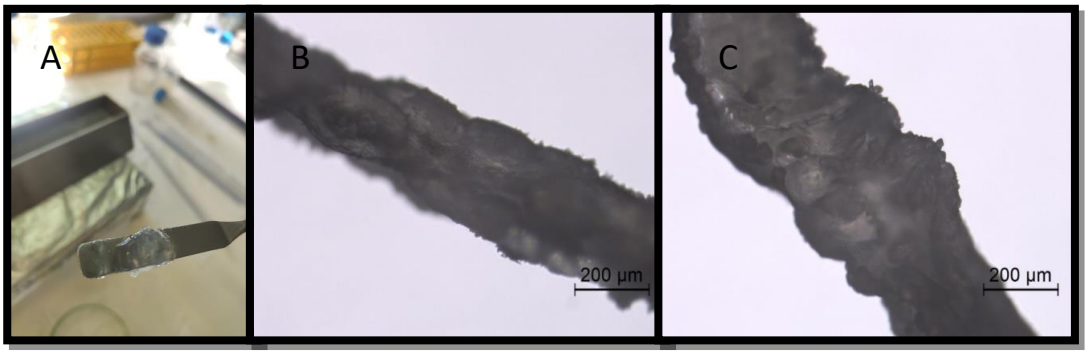

Figure 8: Fibre's optimizations. A) Appearance of the gel-like structure formed after the WS of the first formulation; B) Optical microscopy image of the fibres obtained in 1 M NaOH bath at 3 °C and with 0.41 mm needle. (10x magnification); C) Optical microscopy image of the fibres obtained in 1 M NaOH bath, room temperature and 0.64 mm needle diameter (10x magnification).

Since the previous formulations were not working, the concentrations of acetic acid were optimized, until the solution seemed acceptable for WS.

Therefore, in the following solution, 6 % of acetic acid was used in order to correctly dissolve the CH. This formulation was tested at two different temperatures and in two different baths. The optical microscopy images of the developed fibres are represented in Figure 9 and show the appearance of the fibres obtained by this formulation following different conditions.

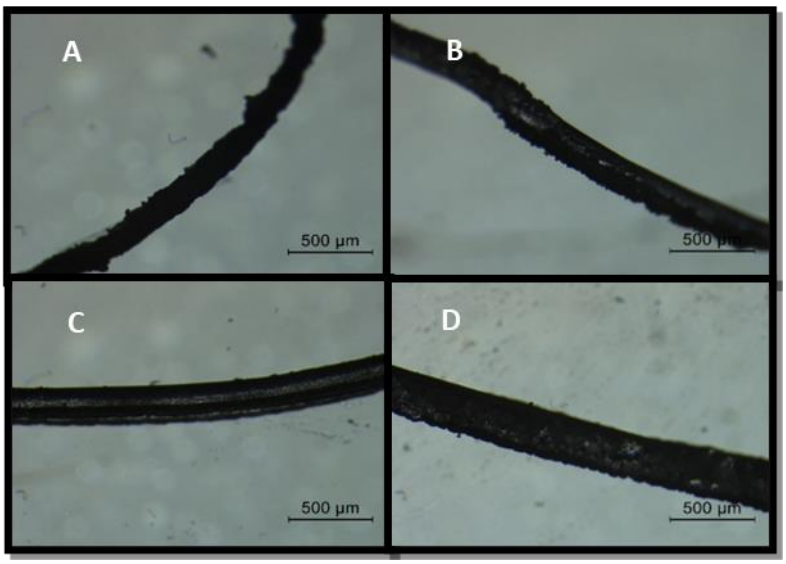

Figure 9: Optical microscopy image of fibres (5x magnification): (A) at room temperature in a 1 M NaOH bath; (B) after fridge in a 1 M NaOH bath; (C) at room temperature in a 2 M NaOH bath; (D) after fridge in a 2 M NaOH bath.

In order to be able to compare the results with another percentage of CH, the possibility of having solutions with 3 % CH, optimized similarly to the previous concentration, was also studied. In this solution, 12 % of acetic acid was used to dissolve correctly the 3 % of CH. This

formulation was then tested at two different temperatures and in two different baths, just like the previous one.

The following images represented in Figure 10 were captured using an optical microscope and represent the morphology of the fibres produced by this formulation.

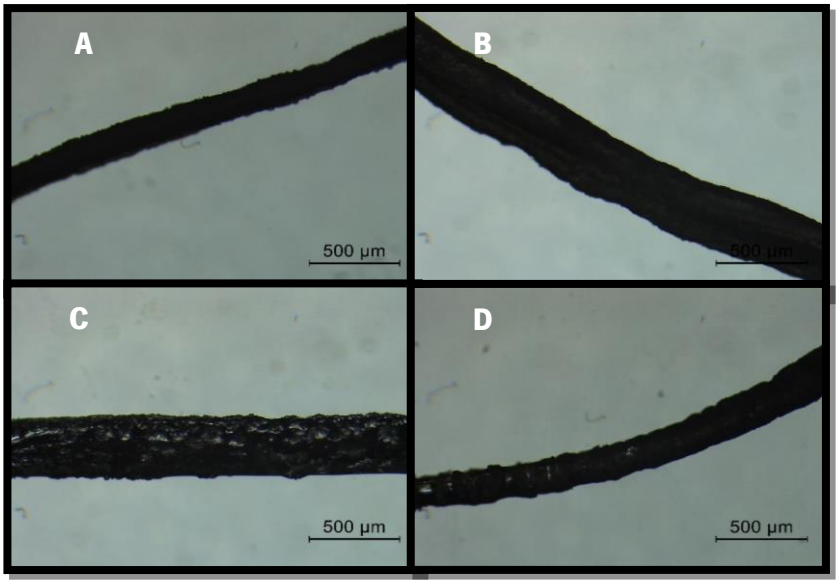

Figure 10: Optical microscopy image of fibres (5x magnification): (A) after fridge in a 1 M NaOH bath; (B) after fridge in a 1 M NaOH bath; (C) at room temperature in a 2 M NaOH bath; (D) after fridge in a 2 M NaOH bath.

As for the fibres tested with 4% chitosan, the corresponding polymeric formulation was unavailable to obtain good results, something that can be justified by the high concentration of chitosan and consequent difficult dissolution of the same, with high viscosity.

Following the collection of all relevant findings, the diameters of the fibres were verified in order to study their homogeneity. Table 10 displays the mean diameters that were obtained, as well as the correspondent standard deviation values.

Table 10: Mean and standard deviation values of the diameters of the fibres obtained

Solution	Mean	Standard deviation
2 % CH with 6 % AcOH aqueous solution – 1 M	175 µm	27.0 µm
2 % CH with 6 % AcOH aqueous solution – 1 M – after fridge	211 µm	22.4 µm
2 % CH with 6 % AcOH aqueous solution – 2 M	***223 µm***	***3.82 µm***
2 % CH with 6 % AcOH aqueous solution – 2 M – after fridge	***292 µm***	***4.96 µm***
3 % CH with 12 % AcOH aqueous solution – 1 M	368 µm	5.68 µm
3 % CH with 12 % AcOH aqueous solution – 1 M – after fridge	***200 µm***	***5.04 µm***
3 % CH with 12 % AcOH aqueous solution – 2 M	370 µm	9.20 µm
3 % CH with 12 % AcOH aqueous solution – 2 M – after fridge	217 µm	17.6 µm

As shown in this table, the three solutions with the best results were the ones marked bold, once they showed a minor value for their standard deviation, showing less structural flaws over the surface of the fibres. Of these three, the one chosen to be used was the 3 % CH with 12 % AcOH aqueous solution since a less concentrated NaOH bath is required for its use. Therefore, the optimized solution of the CH system is a solution with 3 % CH with a 12 % AcOH aqueous solution with low temperature and a 1 M NaOH bath.

4.1.1 CROSSLINKING OF CHITOSAN FIBRES

After these optimizations in order to realize WS, crosslinking methods were used. This technique is commonly used to improve mechanical integrity strength of the fibres. As stated before, three different methods were used. Table 11 shows the resume of the conditions used on all of them:

Table 11: Conditions of the crosslinking of the fibres

Method	Crosslinking agent	Conditions
Vapor deposition: net	5 mL of GTA	Two different temperatures of drying: room temperature or at 50 °C for 1 or 4 hours
	6 mL of GTA	
Vapor deposition: glass Bowl	5 mL of GTA	
	6 mL of GTA	
Bath	Solution with 1 % GTA	4 hours of bath with two different temperatures for drying: room temperature or 50 °C
	Solution with 1 % TPP	
	Solution with 1 % GTA and 1 % TPP	

In the first method, with vapor deposition on the net, the results were not satisfactory as the fibres could not be removed from the net and they appeared to be badly damaged. Despite changing all of the parameters mentioned, this method couldn't reach viable results for the composition of the fibres and that was confirmed by the microscopy analysis of these ones. As shown in Figure 11, all of the fibres presented a large number of defects.

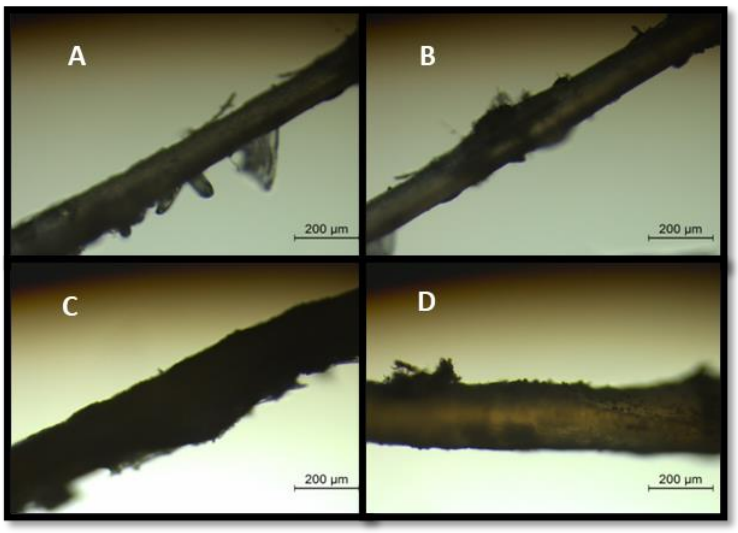

Figure 11: Example of Optical microscopy image (10x magnification) of fibres obtained with net method: A) 5 mL of GTA dried at room temperature for 1 hour; B) 5 mL of GTA dried at 50 °C for 4 hours; C) 6 mL of GTA dried at room temperature for 1 hour; D) 6 mL of GTA dried at 50 °C for 4 hours.

For this reason, this method was discarded and another one was tested. In the second method, instead of placing the fibres on a net, the fibres were placed directly onto the beaker, trying to avoid the defects resulting on its remotion seen before. All the parameters used before stayed the same, in order to compare and try to reach better results. Through microscopy analysis again, it was witnessed that, regardless of the change from net to bowl and although there are small improvements in the results obtained, the fibres obtained were still not satisfactory (Figure 12).

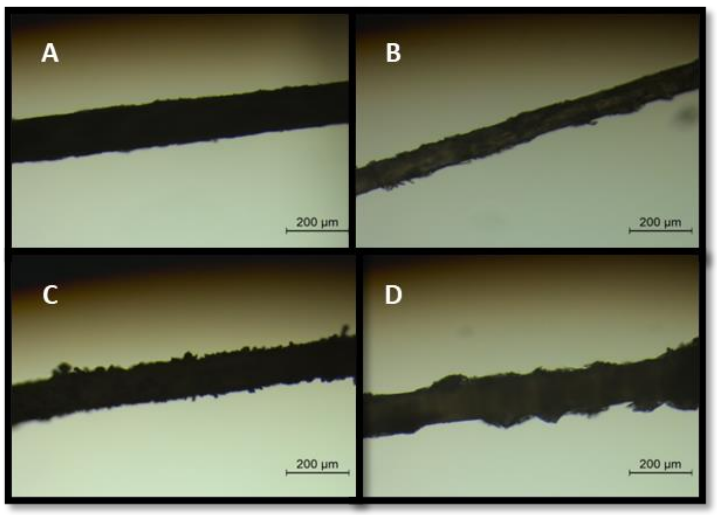

Figure 12: Example of Optical microscopy image (10x magnification) of fibres obtained with glass bowl method: A) 5 mL of GTA dried at room temperature for 1 hour; B) 5 mL of GTA dried at 50 °C for 4 hours; C) 6 mL of GTA dried at room temperature for 1 hour; D) 6 mL of GTA dried at 50 °C for 4 hours.

As a result of the poor results obtained previously, a new method was also tested. In this method, the fibres were immersed in a crosslinking bath. Three different baths were tested, one with GTA, another with TPP and another with a mixture of both. Only in the TPP bath it was possible to acquire results suitable for analysis, since in the other baths the fibres ended up breaking very easily, escaping the expectations of the same ones.

Through a new microscopic analysis illustrated in Figure 13, it was possible to verify that the results obtained by this method were much better than the ones obtained before, with less defects in the fibres. Besides, through the analysis of the average diameters of the fibres presented in Table 12, it was possible to corroborate the previous idea and to choose the best formulation of the bath that would be used from now on.

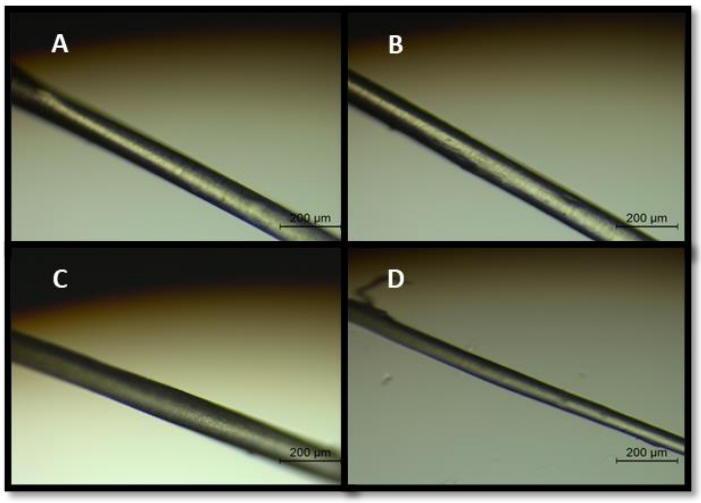

Figure 13: Optical microscopy image (10x magnification) of fibres obtained with bath method: A) and B) 4 h of 1 % TPP bath dried at room temperature; C) and D) 4 h of 1 % TPP bath dried at 50 °C.

Table 12: Mean and standard deviation values of the diameters of the fibres obtained

Fibre diameters at	Mean (µm)	S. Deviation (µm)
Room temperature	114	3.87
50 °C	95	9.34

Thus, as it is possible to analyze through the table above, the smaller standard deviation present in the average of the fibres diameters would be the one resulting from the TPP bath for four hours and subsequent drying at room temperature, leading to the conclusion that it is with this formulation that the fibres with less defects and closer to the best results are obtained.

4.2 CHITOSAN/PEO WETSPUN FIBRES

CH and PEO are two biodegradable polymers that have been widely used for the production of fibres. In fact, several authors have combined these two biodegradable polymers in order to take advantage of the inherent advantages of each one of them, i.e., to combine the bioactivity of CH with the mechanical strength of PEO [118]. Therefore, in this section, the CH/PEO system was optimized. Similarly, to the previous system, at an early stage, the different parameters at the solution and WS process levels were evaluated.

Fibres with a better diameter distribution and apparent morphology than the previous ones were obtained by using 3 %(w/v) CH/PEO (1:1) dissolved in an aqueous solution with 12 % AcOH aqueous solution. A flow rate value of 1 mL/min, a 0.41 mm diameter needle and a coagulation bath of 1 M of NaOH were used. The posterior crosslinking bath used was the one optimized as well: four hours of a TPP bath with drying at room temperature.

4.2.1 PRODUCTION AND OPTIMIZATION OF CHITOSAN/PEO WETSPUN FIBRES

In order to produce CH/PEO fibres several parameters were evaluated and optimized, including pre-processing, percentage and proportion of the polymers, percentage of the solvent, post-processing of the solution mixture (centrifugation and homogenization), order of the addition of the reagents and polymers in the solution.

For this, three solutions were obtained and then centrifuged for 20 minutes at 4000 rpm and cooled after 24 h in the fridge. With these solutions the WS was carried out, maintaining the previously optimized conditions.

First formulation: 1 %(w/v) PEO with 3 %(w/v) CH in a 12 %(v/v) AcOH aqueous solution

Second formulation: 2 %(w/v) PEO with 3 %(w/v) CH in a 12 %(v/v) AcOH aqueous solution

Third formulation: 2 %(w/v) PEO with 3 %(w/v) CH in a 12 %(v/v) AcOH aqueous solution

The microscopic images of the fibres obtained allowed conclusions to be drawn about them, once again helping to verify their diameter variation and surfaces. Thus, in Figure 14 the fibres obtained are represented with 1 %, 2 % and 3 % PEO, respectively. Their mean diameters and standard deviation values are exhibited in Table 13.

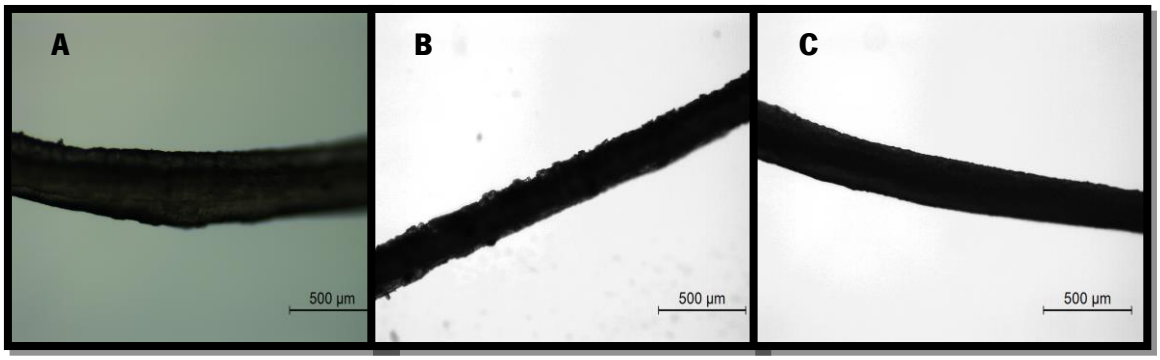

Figure 14: Optical microscopy image of fibres (5x magnification) with: A) 1 % PEO; B) 2 % PEO; C) 3 % PEO.

Table 13: Mean and standard deviation values of the diameters of the fibres obtained

Fibre Diameters of	Mean (µm)	S. Deviation (µm)
1 % PEO 3 % CH	112	7.75
2 % PEO 3 % CH	108	6.32
3 % PEO 3 % CH	105	4.39

With this, it can be seen that, regardless of the value of the percentage of PEO, there is a reduction in the mean value of the fibres' diameter, in comparison to the ones without PEO. For higher percentages of PEO, it can be observed a higher reduction in fibre diameter, as well as a tendency for the standard deviation to be also lower. Regarding their appearance, it can also be seen a surface that seems to be less rough, as well as less brittle and more elastic than the previous ones, confirming the improvement of the physical properties with the addition of PEO.

4.3 CHITOSAN/PVA WETSPUN FIBRES

The PVA polymer may be used in an almost endless number of industries, especially as attention turns away from synthetic materials and toward biodegradable ones. This phenomenon has opened up a wide range of opportunities for such materials because of their environmentally friendly and user-friendly qualities [12].

When combined with polymers like CH, they can provide significant benefits for a variety of applications, so they will also be studied in this article and in this section.

The evaluation of many parameters was done at both the solution and WS process levels. Using 5 %(w/v) PVA with 3 %(w/v) CH mixed in an aqueous solution with a 12 % AcOH aqueous solution, fibres were produced with a better diameter distribution and apparent morphology than the prior ones. A 0.41 mm diameter needle, a 1 M NaOH coagulation bath, and a flow rate of 1 mL/min were employed as well as a posterior crosslinking bath: four hours in a TPP bath, followed by drying at room temperature.

4.3.1 PRODUCTION AND OPTIMIZATION OF CHITOSAN/PVA WETSPUN FIBRES

The pre-processing, percentage and proportion of the polymers, percentage of the solvent, post-processing of the solution mixture (centrifugation and homogenization), and order of the addition of the reagents and polymers in the solution were evaluated and optimized in order to produce CH/PEO fibres.

Once again, three solutions were produced, centrifuged for this at 4000 rpm for 20 minutes, and then chilled in the refrigerator for 24 hours. The solutions produced were the following:

First formulation: 1 %(w/v) PVA with 3 %(w/v) CH in a 12 %(v/v) AcOH aqueous solution

Second formulation: 3 %(w/v) PVA with 3 %(w/v) CH in a 12 %(v/v) AcOH aqueous solution

Third formulation: 5 %(w/v) PVA with 3 %(w/v) CH in a 12 %(v/v) AcOH aqueous solution

The inferences that might be taken about the fibres from their microscopic images helped confirm their surface and diameter variation yet again. As a result, in Figure 15, the produced fibres are shown with, respectively, 1 %, 3 %, and 5 % PVA. Table 14 shows their mean diameters and standard deviation values.

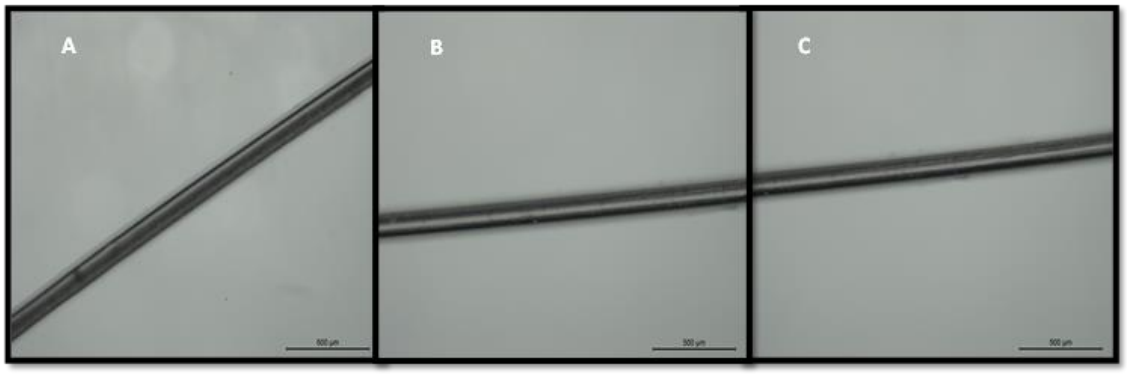

Figure 15: Optical microscopy image of fibres (5x magnification) with: A) 1 % PVA; B) 3 % PVA; C) 5 % PVA.

Table 14: Mean and standard deviation values of the diameters of the fibres obtained

Fibre Diameters of	Mean (µm)	S. Deviation (µm)
1 % PVA 3 % CH	123	5.24
3 % PVA 3 % CH	117	5.14
5 % PVA 3 % CH	103	3.94

As previously seen in CH/PEO system, regardless of the value of the percentage of PVA, there is a reduction in the mean of the diameter of the fibres, in comparison to the ones without PVA, being noticed as well that once again, for higher percentages of polymer added it can be observed a higher reduction in fibre diameter, as well as a tendency for the standard deviation to be also lower. In comparison with the CH/PEO results, it can be seen that value for the standard deviation is better once it is lower.

By looking at the images it can also be seen some less defects, showing that in this chapter the system of CH/PVA might be superior. However, these conclusions were not decisive

for choosing what system should be used, once the most important parameters are the mechanical properties of this system and the incorporation of MNPs in these fibres.

4.4 Ferromagnetic NPs

As stated before, ferromagnetic NPs are really promising NPs especially due to their biocompatibility and stability, biodegradability, ease of surface modification and functionalization [55][56]. In this work, ferromagnetic NPs were produced in order to be incorporated onto the fibres. After this, a fibrous structure with these NPs was developed, making it possible to act as a drug delivery system for hyperthermia therapy for cancer.

In order to produce these NPs, as already highlighted, methods previously written in an article done by César A. Henriques *et al.* were followed [126].

4.4.1 Ferromagnetic NPs Produced - Magnetic Characteristics and STEM Analysis

After following the mentioned protocol, the final solution resulting from the co-precipitation process was obtained with the suspended NPs. Using a magnet, it was also possible to instantly verify the magnetic response capacity of the same solution as the magnet was moved forward as shown in the sequence of Figure 16.

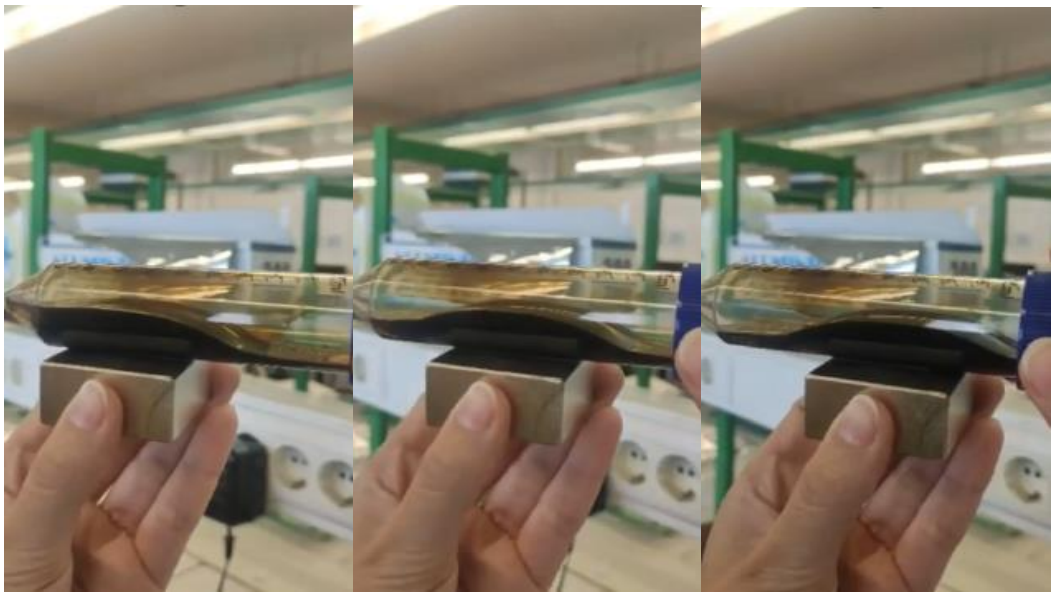

Figure 16: Magnetic response from the obtained NPs' solution to the movement of a magnet.

In order to characterize the NPs obtained, they were analyzed via STEM, presenting the results in Figure 17. According to the analysis performed by TEM in the article previously followed for the production of these particles, these should have a size of approximately 8.3 nm [126]. However, since the equipment available for analysis in this case was a STEM with a minimum measurement until about 9 nm, it is possible that the NPs in question are also comprised between these sizes. As for the dispersion, it is possible to verify that there is not much agglomeration, which shows once again that it is possible to have a good stability, as also mentioned in the previous article. Related to the shape, it shows almost a spherical shape. These characteristics can be proven by the previously mentioned article and by studies related to the production of ferromagnetic NPs [113][129]–[131].

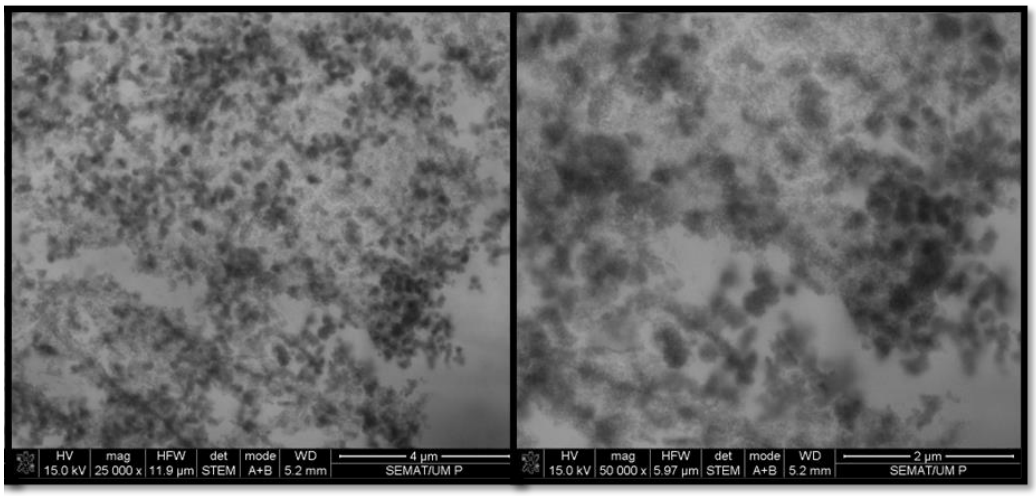

Figure 17: STEM images of ferromagnetic NPs.

After checking its activity, this solution was placed in an oven for 3 hours at 150 °C so that all excess solvents could be evaporated. At the end of this time, the NPs were dried and once again they showed magnetic characteristics - Figure 18 -, proving that the drying process did not affect them, and that they can be used for the intended application.

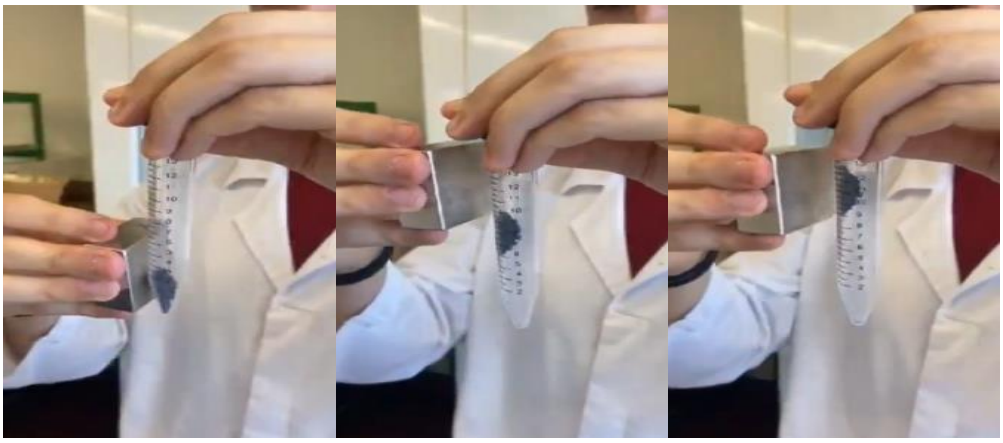

Figure 18: Magnetic response from the obtained dried ferromagnetic NPs to the movement of a magnet.

4.5 Fibres with Ferromagnetic NPs

With the CH/PEO and CH/PVA systems optimized and after the desired MNPs were obtained a new step emerged. In this step the dissolution of the MNPs in the optimized solutions to make the NPs integrate the fibres was the goal.

To reach this goal, combinations including the previously optimized solutions and various ferromagnetic nanoparticle concentrations were tested, trying to obtain the final solution. The combinations tried out are expressed in following Table 15:

Table 15: Combination of different solutions and NPs percentages

Solutions	% NPS
3 % CH 3 % PEO	0.5
	1
	2
3 % CH 5 % PVA	0.5
	1

Images of the different fibres with different percentages of NPs are shown in Figure 19. As it is visible, all fibres presented a good homogeneity in diameters, presenting few defects, as

expected, given the previous optimization. Since at this stage it was important to analyze the results obtained in more detail in order to choose the final solution that would serve as the basis for the final system, mechanical tests were performed, opting for the solution that stood out in that sense.

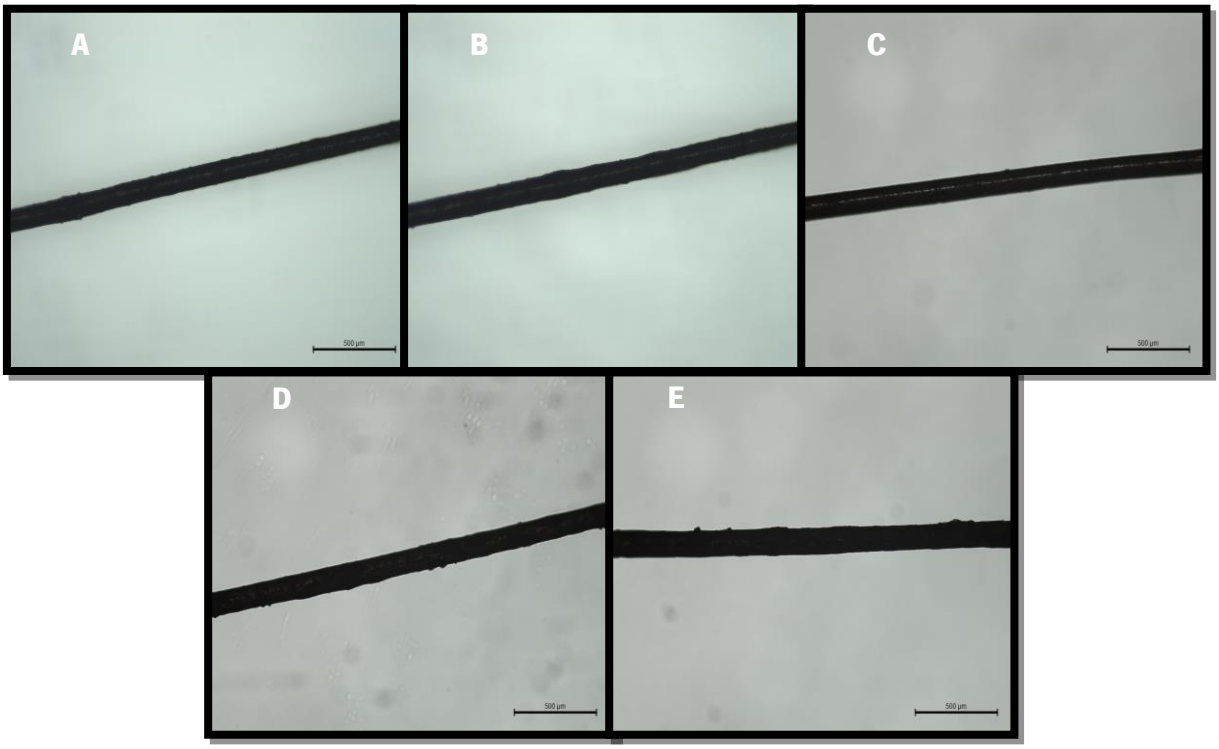

Figure 19: Optical microscopy image of fibres (5x magnification). PEO Fibres with: A) 0.5 % MNPs; B) 1 % MNPs; C) 2 % MNPs. PVA Fibres with: D) 0.5 % MNPs; E) 1 % MNPs.

4.5.1 Mechanical Tests

After the production of all the fibres resulting from all the different solutions by wetspinning, it was proceeded to the mechanical analysis of the fibres, since, as previously reported, after the optimization of the solutions, the microscopic analysis previously done is not very conclusive and it is not possible to detect such big differences as it was possible to do by comparing the diameters of the fibres. Therefore, and because it is also very important for the

final structure, the fibres were analyzed using mechanical tests. Previous samples without NPs were also analyzed to act as a term of comparison and control.

In these mechanical tests different properties such as Young's modulus, elongation at break and maximum stress were determined. The results are shown in Table 16.

Table 16: Mechanical results of different fibres with different percentages of NPs

Solutions	% NPS	Max. Tension (MPa)	Deformation on Max. Tension (%)	Breaking Point (MPa)	Deformation at break (%)	Young's modulus (GPa)
3 % CH 3 % PEO	0	2.84E-2	1.08	0.17E-2	1.59	0.38E-4
	0.5	6.80E-2	6.03	1.63E-2	6.93	0.35E-4
	1	7.01E-2	4.06	2.7E-2	6.39	1.00E-4
	2	7.88E-2	5.82	5.41E-2	6.67	1.00E-4
3 % CH 5 % PVA	0	5.65E-2	1.65	0.17E-2	6.48	0.46E-4
	0.5	5.64E-2	3.04	2.59E-2	3.26	1.00E-4
	1	6.04E-2	1.89	3.40E-2	2.15	1.00E-4
	2	-	-	-	-	-

Analyzing the results, in most cases, the higher the increase in the percentage of NPs, the higher are the values for the characteristics analyzed in this table. For example, with the addition of NPs in the fibres with PEO, these fibres start to present higher maximum stress values, reaching 7.88E-2 MPa with 2 % NPs, which corresponds to an increase of approximately 177 % in relation to the fibres without NPs, which is quite a significant increase. Also, in breaking point and Young's modulus there were considerable increases, reaching the 5.41E-2 MPa and 1.00E-4 GPa, correspondingly. All this also happens for the fibres with PVA, where the maximum result for the maximum stress was 6.04E-2 MPa, an increase not so significant but still 7 %. The Young's modulus and the breaking point also improved to 3.40E-2 MPa and 1.00E-4 GPa. Before the addition of ferromagnetic NPs, the best mechanical properties were found in PVA fibres, but with the addition of these NPs, PEO fibres showed a big improvement, outperforming the PVA ones. In an article by Brüggemann *et. al* where chitosan fibers with MNPs were developed, this behavior of fibers with and without MNPs was also verified [132]. Although the values obtained for the properties were lower then the ones obtained in the article, the fibers produced had a larger diameter, which influences all these aspects. Nevertheless, with these comparisons it is possible to say that results obtained corroborate the idea that these NPs can not only conceive

magnetic properties but also mechanical reinforcement properties to the fibres in question, saving a rare exception for the fibres produced with PVA and 2 % NPs, as they were so brittle that it was impossible to perform their tests.

Concluding about the best fibres, it can be seen that the ones that presented the best results were the fibres with PEO and 2 % NPs, opting then for this formulation for all the rest of the work, namely the production of the final structure.

4.5.2 ATR-FTIR Analysis

To characterize the CH/PEO nanofibres obtained and to study the possible interactions between the polymers, ATR-FTIR analysis was performed. Figure 20 presents the ATR-FTIR spectrum of the CH/PEO fibre without NPs.

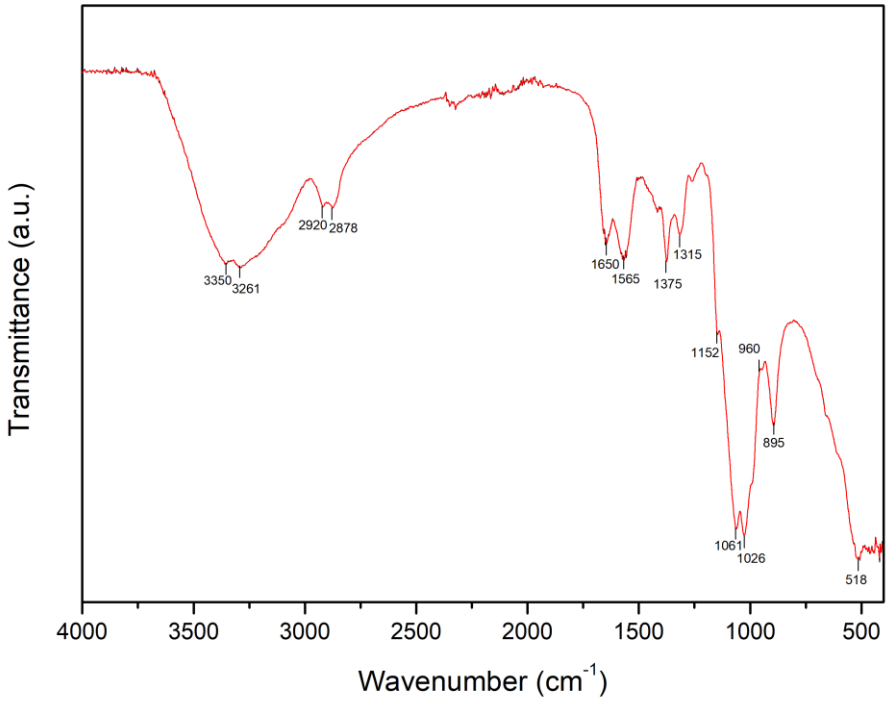

Figure 20: ATR-FTIR spectrum of CH/PEO fibres.

Hence, related to CH, it is possible to observe several bands in the spectrum characteristics of this polymer, including a band in the region between 3200 and 3500 cm^{-1}

corresponding to the stretching of N-H and O-H groups and an absorption band at 2921 cm^{-1} attributed to asymmetrical stretching of CH_2 [133][131].

Additionally, there is the presence of the typical bands at 1650 and around 1555 cm^{-1}, which correspond to amide I (C=O stretching) and amide II (N-H bending), respectively. The band at 1375 cm^{-1} is attributed to symmetric deformation of the CH_3 bond [134][135].

Finally, the bands at 1146, 1061, 1026 and 895 cm^{-1} are a result of the saccharide structure of CH, where the band at 1150 cm^{-1} is assigned to the symmetric stretching of the C-O-C bond, while the bands located at 1057 and 1026 cm^{-1} are a result of the stretching vibrations of the C-O bond [136][137].

In relation to PEO, the spectrum shows the presence of several bands, the most characteristic ones being the band at 2878 cm^{-1} attributed to the C-H bonds; the bands at 1146 and 1061 cm^{-1} that correspond to the vibrations of bond elongation in C-O-C and the band at 960 cm^{-1} that is indicative of the C-C bonds [138].

Thus, the characteristic bands of both polymers are visible. In order to confirm the possible interaction between CS and PEO, it is worth noting the slight shift observed in the CS amide group, which according to the literature would be around 1555 cm^{-1}, but that in this case has shifted to higher wave numbers, possibly indicating the formation of hydrogen bridges between the two polymers when PEO is introduced [139].

4.5.3 SEM AND EDS ANALYSIS

SEM was used to analyze the morphology of the fibres with and without NPs. By comparing the figures obtained with this technique, it can be seen that both appear to have compact surfaces. However, in Figure 21A a super regular surface can be seen, while in Figure 21B, there is a surface with particles scattered on it.

To verify whether these particles resulted from the functionalization of the fibres with the synthesized NPs, the EDS technique was also used. Table 17 illustrate the findings of the study of fibres without and with MNPs, showing the atomic quantification of which component in the sample. By analyzing this table, it can be seen a major change on the composition of the fibres with or without MNPs based on the inclusion of iron, that is the main source on the production of MNPs in this study. This fact explains why the fibres may exhibit magnetic properties and

when combined with the prior FTIR study results, makes plausible to infer that CH/PEO fibres with and without MNPs were efficiently created.

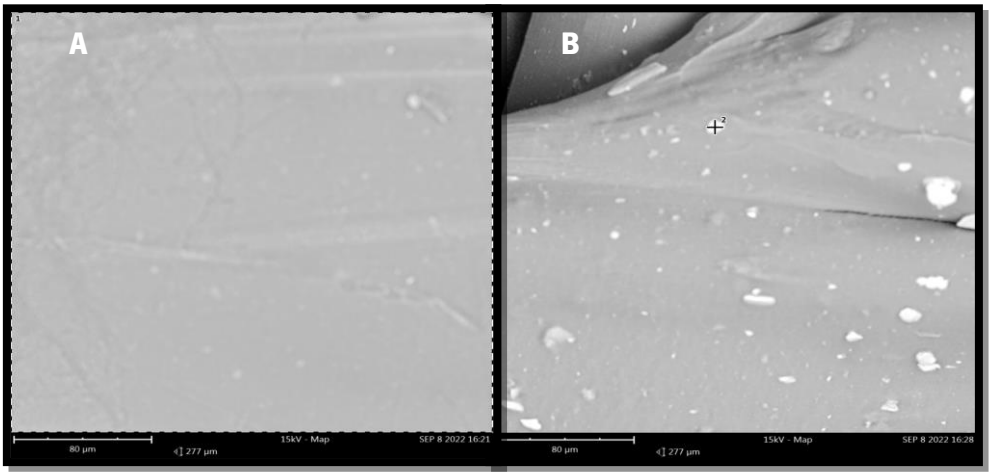

Figure 21: SEM images of A) fibres without NPs; B) fibres with NPs.

Table 17: EDS analysis showing atomic quantification of the fibres

	Atomic quantification					
Fibres	Silicon	Oxygen	Sodium	Carbon	Phosphorus	Iron
Without MNPs	0.31	44.93	10.9	39.87	3.99	0
With MNPs	0.37	42.03	6.58	35.03	2.37	13.62

4.5.4 FIBRES FUNCTIONALIZED WITH FERROMAGNETIC NPS - TGA ANALYSIS

To evaluate the effect of the incorporation of MNPs in the thermal stability of CH/PEO nanofibres and in order to estimate the residual weight of the untreated (without NPs) and treated (with NPs) samples, and therefore, infer about the percentage of NPs deposited on fibres, TGA analysis was performed. The thermal degradation curves obtained are shown in Figures 22 and 23.

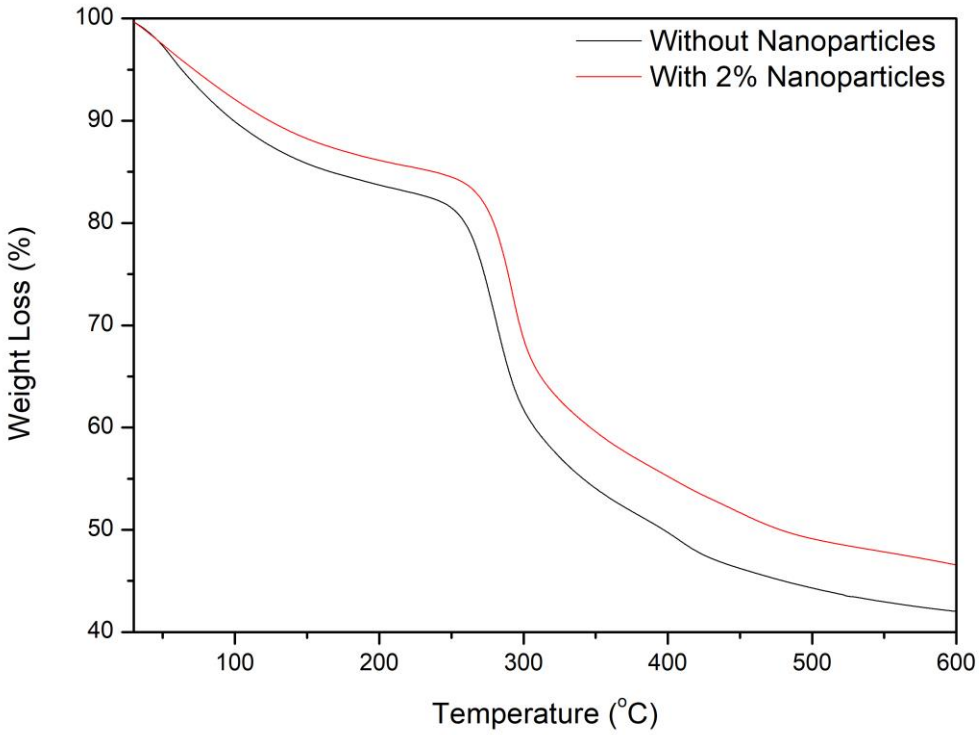

Figure 22: TGA curves obtained for fibres with or without NPs.

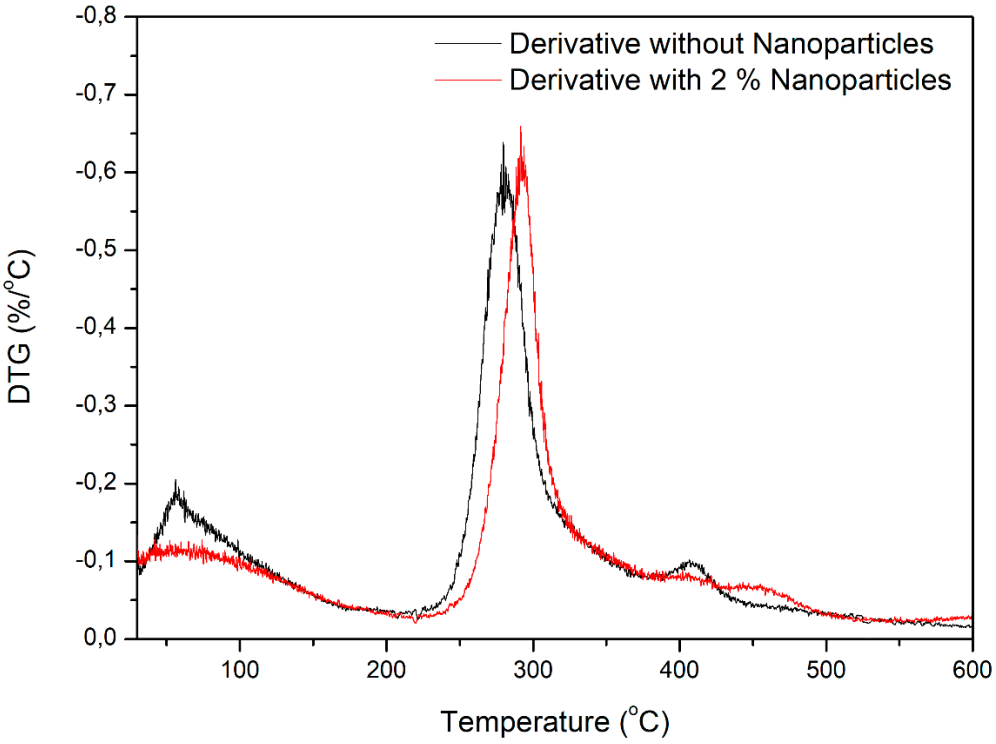

Figure 23: DTG curves obtained for fibres with or without NPs.

By observation of Figure 22, it is visible that for both TGA curves there's an initial mass loss occurs, between 40 °C and 150 °C, related to the evaporation of absorbed water and other volatile compounds [112]. The TGA and DTG curves also show two main mass loss steps: the first occurs between 250 °C and 300 °C, and corresponds to the degradation of CH, the second step is related to the degradation of PEO and occurs between 360 °C and 420 °C, confirming the presence of these two polymers in CH/PEO nanofibres.

By observation of the DTG graph these previously mentioned peaks can also be identified and another one in the red band (with 2 % NPs) can also be identified. This peak, at around 400-500 °C band is associated with the phase transformation of Fe_3O_4-Fe_2O_3 as already mentioned in an article by Nigam S. *et al.,* showing once more the particles included on the fibres [131].

Thus, through this analysis, the success of the incorporation of NPs in CH/PEO nanofibres was proven and, at the same time, it was also verified that the incorporation of these NPs in CH/PEO nanofibres confers a higher resistance to thermal degradation, as their final value remains higher than the value presented by the fibres without MNPs.

4.5.5 Swelling and Degradation Tests

Swelling and degradation tests were performed to the fibres with the best mechanical properties to study and understand how fibres would respond to being incubated for a long period of time in water. As seen in Table 18, the solution without NPs had the highest swelling degree (315 ± 5.49 %) and in vitro degradation (26.6 ± 1.69 %) after 24 h. The fibres with MNPs reached minor values.

As is generally known, a more hydrophilic material may absorb more water, resulting in larger swelling degrees and consequently altering the degradation rates of the material's systems. For the fact that PEO and CH are two hydrophilic polymers and CH presents well deal of interests for hydrogen bonding with water molecules, the results found in fibres without NPs for swelling are according to the literature. As the swelling is higher in these fibres, when they are subjected to degradation tests their volume will be higher and therefore higher will be the chance of more mass loss and consequently higher degradation [140][141][142].

With the addition of NPs to the fibre matrix, the fibres tend to become more filled and, consequently, there's results like the reduction of porous that were present before and thus decreases the volume of fluid absorbed, favoring less swelling and less degradation [141].

Having said this, it is possible to state that the incorporation of these NPs is satisfactory, as it allows the fibre structure to be more stable.

Table 18: Swelling and degradation tests results for fibres

Fibres	**Swelling degree (%)**	***In vitro* degradation (%)**
3 % CH PEO 3 %	315 ± 5.49	26.6 ± 1.69
3 % CH PEO 3 % with 2 % Ferromagnetic NPs	243 ± 2.39	12.2 ± 1.28

4.6 PRODUCTION OF THE FIBROUS STRUCTURES

MNPs can enter the body through systemic circulation and accumulate at tumor locations, or they can be injected directly into the tumor. However, particles injected intravenously are quickly covered by circulation components such as plasma proteins. The adsorption of proteins on the particle surface, termed opsonization, facilitates phagocytosis. Furthermore, most intravenously injected NPs are recognized by the body as "foreign bodies" and are quickly eliminated by circulating monocytes or fixed macrophages [143]. To avoid reticuloendothelial system activity, particle size must be controlled, else they would aggregate and have a short half-life in the blood circulation. The magnetic particles utilized are very tiny (dozens of nanometers) and, consequently, are easily taken away by blood flow and disseminated to different organs or tissues during hyperthermia therapy. To address these issues, a polymeric fibrous matrix is proposed for accurate administration of a magnetic material to the tumor site via a surgical or endoscopic technique for localized magnetic hyperthermia treatment. Diverse structures might lead to radically different consequences, ensuring or not, the success of the same [144].

In this case, the structure developed needed to be ready to cover up a tumor. In order to do so, and considering that tumors have irregular shape, the structure to be developed had to be like a net that would allow the whole tumor to be involved, and therefore flexibility and malleability were indispensable. These two conditions would also be important to define an easier means of administration such as a biopsy tube [82].

To meet these expectations and to produce the structures in question, three different methods were tested.

4.6.1 METHODS FOR FIBROUS STRUCTURES

The methods used and the results obtained are expressed in the following Table 19 and Figure 24:

Table 19: Results for every method used to create fibrous structures

Method	Description	Results
Weaving	In this method, the fibres were used after dried. A technique called weaving was used, wich is based on interlacing two sets of yarns so that they cross each other, normally at right angles.	This method didn't work as the fibres obtained had not enough tension to stay crossed with each other.
Directly in the crosslinking bath	in this method, after obtaining the fibres by wetspinning, an attempt was made to make a net structure by overlapping the fibres one on top of the other directly in the crosslinking bath.	This method didn't work as the fibres were stable enough to create a well shaped structure.
After the crosslinking bath	In this method, after the obtaining the fibres and after diving them in the crosslinking bath for 4 h, the structure was made by overlaping the fibres and leave them to dry at room temperature.	This method had the better results, being able to produce a good structure.

As the last method was the only method that presented satisfactory results, this was the method used for the production of the remaining structures used in this work.

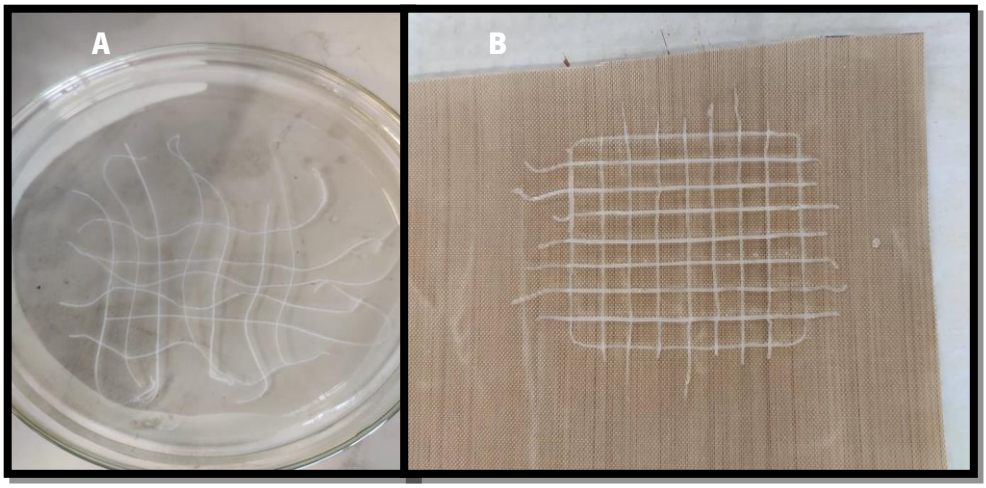

Figure 24: Methods used to produce fibrous structures: A) Directly in the crosslinking bath; B) After the crosslinking bath.

4.6.2 SEM Analysis And Magnetic Characteristics Of The Structures Produced

Using the method previously described, different structures were then produced based on the previously selected formulation: CH/PEO with 2 % MNPs. Structures without the NPs were also made in order to serve as comparison to the previously described ones for mechanical, swelling and degradation tests.

Figure 25 represents the structures obtained without NPs and Figure 26 the structures with 2 % MNPs.

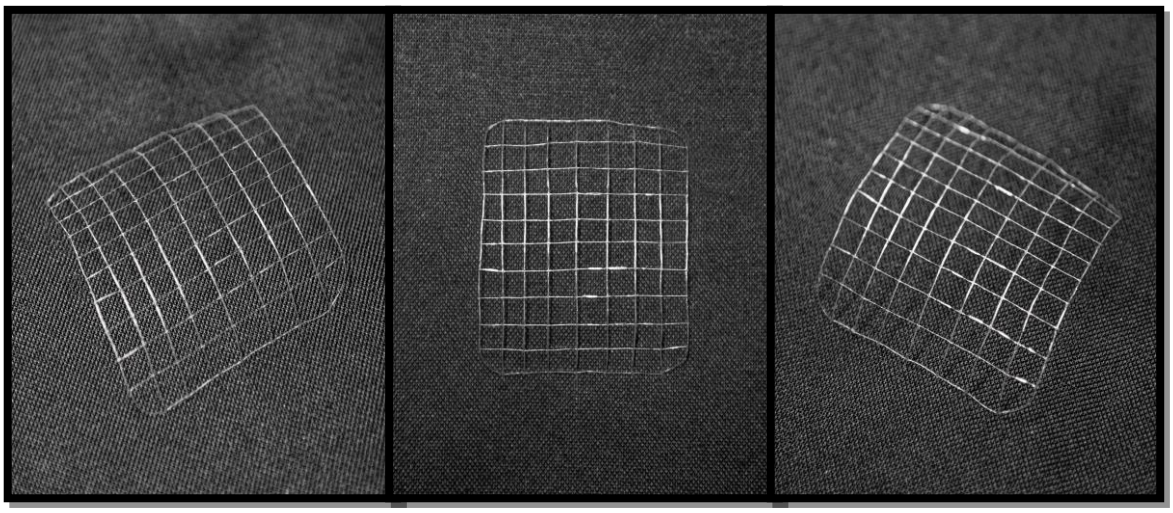

Figure 25: Structures produced with CH/PEO system without MNPs.

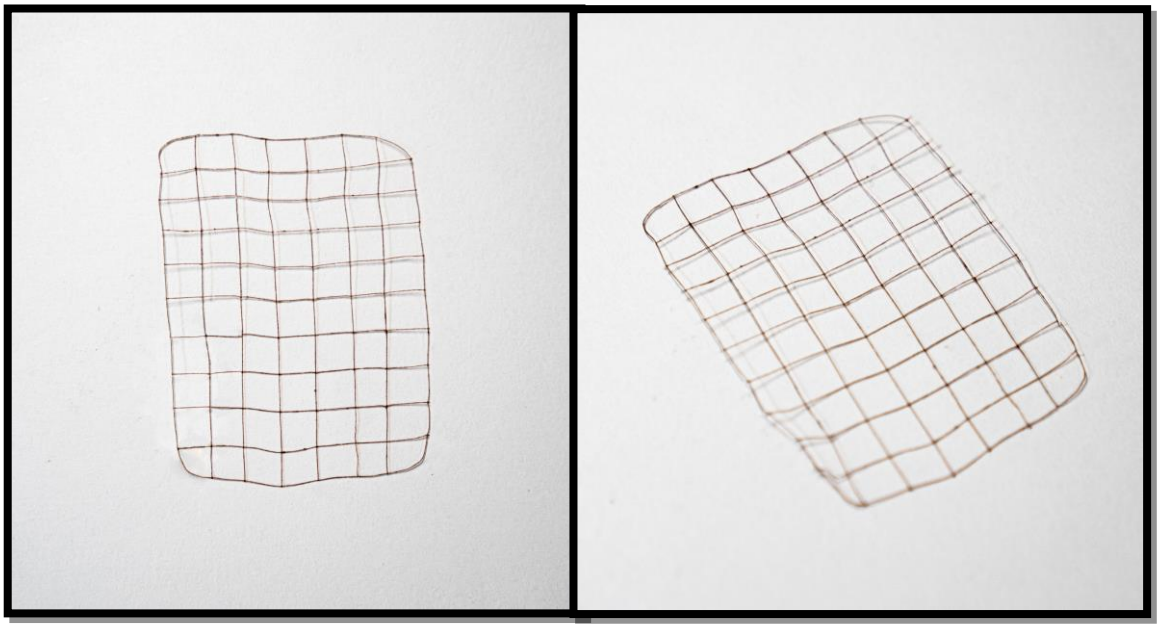

Figure 26: Structures produced with CH/PEO system with MNPs.

It is possible to verify from the figures that well defined structures were obtained, without major defects to the naked eye. As for their color, it can be seen that the structures with NPs acquired an orange color resulting from the iron solutions used in the production of the NPs, unlike those without NPs, which present a white color.

To be able to dimension and to really understand if there are enough defects and the appearance of the structure in the joints, the SEM analysis of the joints in the structures with MNPs was carried out. Thus, according to Figure 27 it can be seen that the structure of fibres with MNPs present a diameter always around 100 nm as previously mentioned with few defects and that the overlapping fibres are well bonded and even seem to have fused together after drying, proving a good optimization of the solution and an effective method of processing these structures. Also, the visual appearance is again similar to those obtained previously for the fibres with MNPs, and so surely if a new EDS analysis were performed it could be once again verified the presence of the iron ion in these structures.

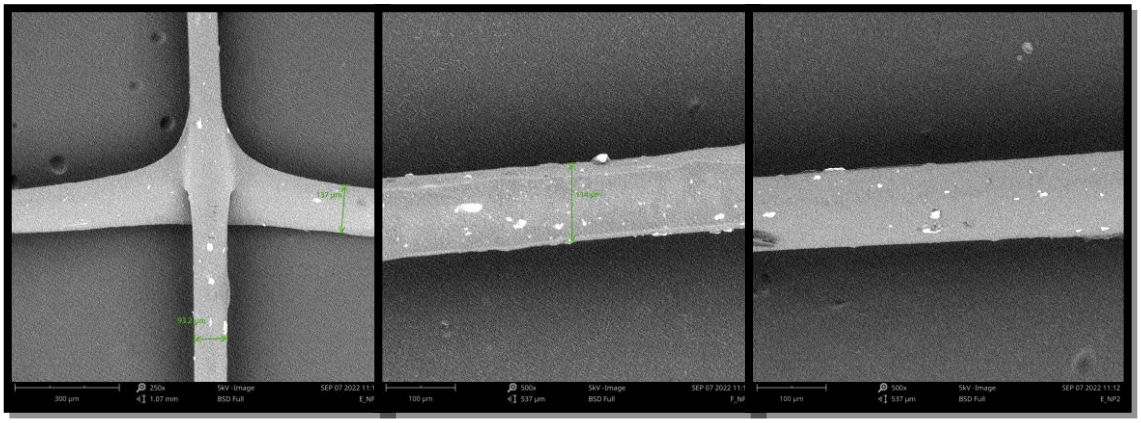

Figure 27: SEM images of the fibre structures with MPNs: joints and fibres present in it.

After this analysis, it was important to understand once again if, this time in structure, the magnetic properties of the MNPs were maintained, making the structure also responsive to magnetic stimulations and with a good and successful incorporation of the NPs. That said through exposure to a magnet again, the structures were quickly attracted by the magnet, showing magnetic field response behavior and potential for remote manipulation of these under a controlled magnetic field, as it is shown in Figure 28. In other articles, Kim *et al.* and Wang *et al.* also performed these tests, concluding that these structures were correctly functionalized with MNPs [87][92].

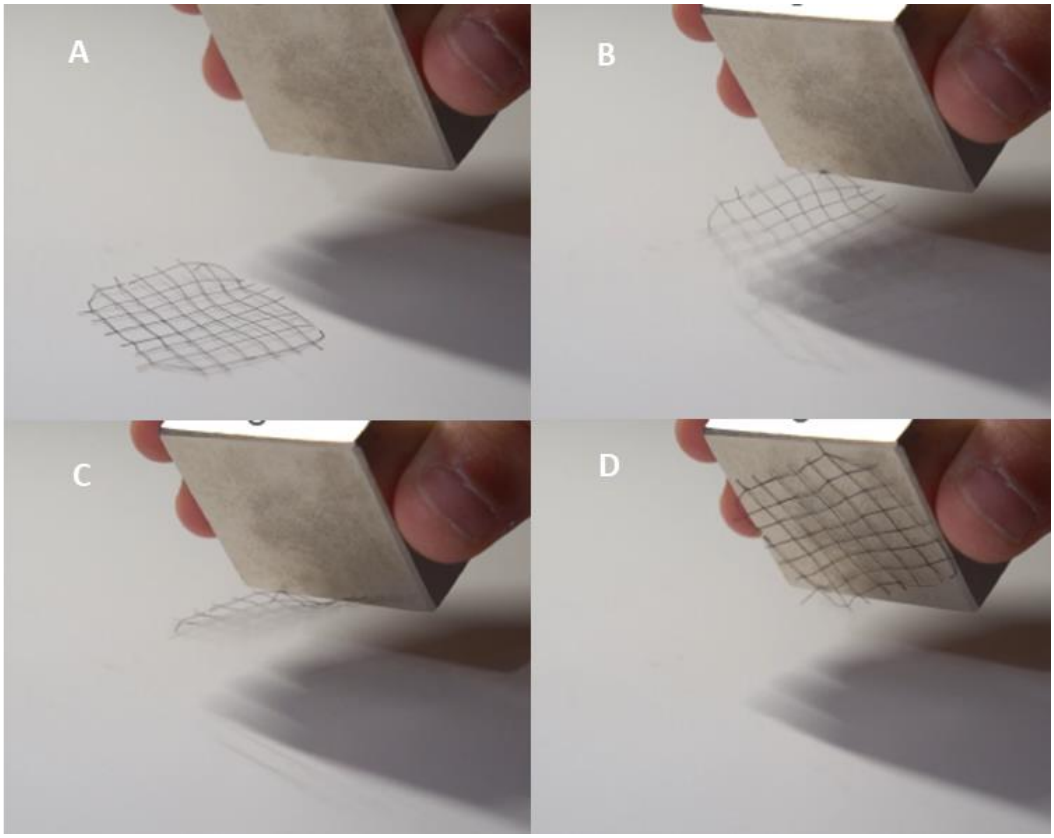

Figure 28: Illustration of the magnetic properties of the structures developed with MNPs: A) Magnet near the structure; B) and C) Structures attaches to the magnet; D) Structure in full contact with the magnet.

4.6.3 Swelling And Degradation Tests

Swelling and degradation tests were performed again to the structures this time to see if the respond would corroborate the results obtained before. The results on Table 20 are essentially comparable, indicating that without NPs, there is a larger proportion of swelling, which corresponds to a higher percentage of degradation. It is also feasible to check an agreement in the values, with both being near to the previously acquired values. It should be noted that in the structure with NPs, there is still a reduction in the percentage of swelling and degradation, which, while tiny, may demonstrate a benefit of the junction of fibres, making its degradation more difficult.

Table 20: Swelling and degradation tests results

Structures	**Swelling degree (%)**	***In vitro* degradation (%)**
Without Ferromagnetic NPs	387 ± 3.56	32.5 ± 4.16
With 2 % Ferromagnetic NPs	221 ± 4.12	14.1 ± 7.83

4.6.4 MECHANICAL TESTS

As regards the mechanical tests performed on the structure, the expected improvements of all the characteristics in relation to those previously calculated with only fibres were proven. Thus, to compare the results obtained in structures, mechanical tests to structures with and without NPs with the optimized solution were performed.

Table 21 shows the values obtained. The addition of NPs resulted in a 12 % increase in the maximum tension that the material can be subjected until rupture. The breaking point and Young's modulus also increased by 61 % and 30 % respectively, but the deformation at break was reduced by 25 %. Since the structures obtained were very similar in relation to its form, this reinforcement effect is due purely to the addition of the stronger and stiffer magnetite particles. These results are equally seen in another study, made by Miyauchi *et al.*, where Polyvinylpyrrolidone/PEO fibres with high concentrations of ferromagnetic and superparamagnetic NPs were developed. In this study, it was noticed that the inclusion of 10 % wt magnetite particles resulted in an increase in breaking point (+41 %) and Young's modulus (+33 %), but a decrease in elongation at break (-41 %). The decrease in elongation at break with higher particle loading was interpreted as being due to different abilities of the fibres to allow fibre necking to occur. This necking phenomenon is gradually restricted with increasing particle content which leads to these results [88].

Table 21: Mechanical Results of structures of fibres

Solutions	Max. Tension (MPa)	Deformation on Max. Tension (%)	Breaking Point (MPa)	Deformation at break (%)	Young's modulus (GPa)
3 % CH 3 % PEO Structure	0.476	10.0	0.112	24.5	0.767E-3
3 % CH 3 % PEO 2 % MNPs Structure	0.534	5.65	0.181	19.6	1.00E-3

5 CONCLUSIONS

This work aimed to develop a localized drug delivery fibrous system with ferromagnetic NPs using the WS process with possible application in the treatment of cancer by magnetic hyperthermia. Hence, a fibrous structure with ferromagnetic NPs was produced with biodegradable polymers by wetspinning. In first instance, CH, CH/PEO and CH/PVA solutions were optimized along with the wetspinning parameters: 1 M NaOH coagulation bath, 1mL/min flow rate and 0.41 mm diameter needle. The crosslinking bath was also optimized, testing three different methods in which the best ones were obtained with a bath of 1 % TPP for 4 h. By microscopic analysis it was also possible to ascertain that the best results resulting from the optimization of the polymeric solutions were obtained with: a solution of 3 % CH 3 % PEO in 12 % acetic acid aqueous solution and a solution of 3 % CH 5 % PVA with a 12 % acetic acid aqueous solution.

After this, a protocol to produce MNPs was followed, obtaining them. By STEM it was found that these possibly comprised below 9 mm with good dispersion and a spherical shape similar to those described in other papers.

The MNPs were then added to the previously optimized solutions, and these were further optimized, varying the concentration of NPs between 0.5-2 %.

Through mechanical tests it was possible to decode the best final formulation, which was the formulation with 3 % CH 3 % PEO 2 % MNPs in a 12 % acetic acid aqueous solution. In order to confirm the correct formulation of the fibres and the presence of MNPs in them, ATR-FTIR, EDS and TGA analysis of the fibres were performed. In these it was possible to confirm the presence of characteristic groups of the polymers used in the solution and also iron, corresponding to the correct incorporation of MNPs.

This final formulation showed not only better mechanical aspects but also magnetic properties when subjected to a magnetic field generated by a magnet. Furthermore, when subjected to swelling and degradation tests, the fibres produced by this formulation showed improvements when MNPs were present, leading to a lower swelling and consequently, to a lower mass loss, i.e., lower degradation.

To produce the desired final structures (a network that could wrap a tumor), three different methods were tested. For this purpose, the method that produced the best results was the method in which the fibres were overlapped by each other in oriented directions after the crosslinking bath. After being dried, swelling, degradation and mechanical tests were carried out

again. Again, the structures with MNPs showed better results, showing lower swelling and degradation values compared to the structures without NPs. Adding to this, it was possible to verify that the addition of MNPs resulted in a 12 % increase in the maximum tension that the material can be subjected to until rupture and that the breaking point and Young's modulus also increased by 61 % and 30 % respectively.

In conclusion, the wetspinning process presents a high potential for the production of nanometric scale fibres, allowing, through the conjugation of the different parameters involved, the production of fibre structures with a good morphology and quite regular diameters. The most promising polymeric system developed was the one composed by CH and PEO, where was gathered the largest set of characteristics for the application in question. Thus, the structures developed using the biodegradable polymers CH and PEO, with MNPs incorporated may come to represent promising systems to be used as treatment for cancer.

6 FUTURE WORKS

With the end of the research project, it is understood that there are still procedures to be performed in order to meet all the essential conditions to obtain a structure capable of being used as cancer treatment. In fact, it would be interesting to study the incorporation of more percentages of MNPs and different structural forms for the arrangement of fibres, in order to obtain better mechanical properties. Moreover, and taking into account that one of the essential requirements of this kind of treatment, it would also be essential to perform cytotoxicity and biocompatibility tests and to characterize in a more detailed way all the magnetic characteristics around the structure, in order to obtain more satisfactory results and prove the good performance of the application.

REFERENCES

[1] J. Ferlay *et al.*, “Cancer statistics for the year 2020: An overview,” *Int. J. Cancer*, vol. 149, no. 4, pp. 778–789, 2021, doi: 10.1002/ijc.33588.

[2] I. Dagogo-Jack and A. T. Shaw, “Tumour heterogeneity and resistance to cancer therapies,” *Nature Reviews Clinical Oncology*, vol. 15, no. 2. Nature Publishing Group, pp. 81–94, Feb. 2018, doi: 10.1038/nrclinonc.2017.166.

[3] C. Pucci, C. Martinelli, and G. Ciofani, “Innovative approaches for cancer treatment: Current perspectives and new challenges,” *ecancermedicalscience*, vol. 13. ecancer Global Foundation, Sep. 2019, doi: 10.3332/ecancer.2019.961.

[4] A. Chicheł, J. Skowronek, M. Kubaszewska, and M. Kanikowski, “Hyperthermia - Description of a method and a review of clinical applications,” *Reports of Practical Oncology and Radiotherapy*, vol. 12, no. 5. Great Poland Cancer Center, pp. 267–275, 2007, doi: 10.1016/S1507-1367(10)60065-X.

[5] W. C. Dewey, L. E. Hopwood, S. A. Sapareto, and L. E. Gerweck, “Cellular Responses to Combinations of Hyperthermia and Radiation 1,” 1977.

[6] L. Roizin-Towle, J. P. And, and B. S. Pirro, “THE RESPONSE OF HUMAN AND RODENT CELLS TO HYPERTHERMIA.”

[7] S. Y. Lee, G. Fiorentini, A. M. Szasz, G. Szigeti, A. Szasz, and C. A. Minnaar, “Quo Vadis Oncological Hyperthermia (2020)?,” *Frontiers in Oncology*, vol. 10. Frontiers Media S.A., Sep. 2020, doi: 10.3389/fonc.2020.01690.

[8] K. McNamara and S. A. M. Tofail, “Nanoparticles in biomedical applications,” *Advances in Physics: X*, vol. 2, no. 1. Taylor and Francis Ltd., pp. 54–88, 2017, doi: 10.1080/23746149.2016.1254570.

[9] Y. K. Sung and S. W. Kim, “Recent advances in polymeric drug delivery systems,” *Biomaterials Research*, vol. 24, no. 1. BioMed Central Ltd, Jun. 2020, doi: 10.1186/s40824-020-00190-7.

[10] W. Men *et al.*, “Fabrication of dual pH/redox-responsive lipid-polymer hybrid nanoparticles for anticancer drug delivery and controlled release,” *Int. J. Nanomedicine*, vol. 14, pp. 8001–8011, 2019, doi: 10.2147/IJN.S226798.

[11] J. Zhang *et al.*, “Flexible inorganic core-shell nanofibers endowed with tunable multicolor upconversion fluorescence for simultaneous monitoring dual drug delivery,” *Chem. Eng. J.*, vol. 349, pp. 554–561, Oct. 2018, doi: 10.1016/j.cej.2018.05.112.

[12] P. I. Tarraco, “Polyfvinyl alcohol) with,” pp. 925–934.

[13] M. Krumova, D. López, R. Benavente, C. Mijangos, and J. M. Pereña, “Effect of crosslinking on the mechanical and thermal properties of poly(vinyl alcohol),” *Polymer (Guildf).*, vol. 41, no. 26, pp. 9265–9272, 2000, doi: 10.1016/S0032-3861(00)00287-1.

[14] R. Riva, H. Ragelle, A. Des Rieux, N. Duhem, C. Jérôme, and V. Préat, “Chitosan and chitosan derivatives in drug delivery and tissue engineering,” *Advances in Polymer Science*, vol. 244, no. 1. pp. 19–44, 2011, doi: 10.1007/12_2011_137.

[15] E. A. Yapar and Ö. Inal, “Poly(ethylene oxide)-Poly(propylene oxide)-based copolymers for transdermal drug delivery: An overview,” *Trop. J. Pharm. Res.*, vol. 11, no. 5, pp. 855–866, Oct. 2012, doi: 10.4314/tjpr.v11i5.20.

[16] B. Aslan, B. Ozpolat, A. K. Sood, and G. Lopez-Berestein, “Nanotechnology in cancer therapy,” *Journal of Drug Targeting*, vol. 21, no. 10. pp. 904–913, Dec. 2013, doi: 10.3109/1061186X.2013.837469.

[17] “Types of Cancer Treatment,” *National Cancer Institute*. .

[18] “Getting Photodynamic Therapy,” *American Cancer Society*. .

[19] E. Lima *et al.*, “Quinoline-and benzoselenazole-derived unsymmetrical squaraine cyanine dyes: Design, synthesis, photophysicochemical features and light-triggerable antiproliferative effects against breast cancer cell lines,” *Materials (Basel).*, vol. 13, no. 11, pp. 1–24, 2020, doi: 10.3390/ma13112646.

[20] T. D. Martins *et al.*, “Red and near-infrared absorbing dicyanomethylene squaraine cyanine dyes: Photophysicochemical properties and anti-tumor photosensitizing effects,” *Materials (Basel).*, vol. 13, no. 9, pp. 1–17, 2020, doi: 10.3390/ma13092083.

[21] K. Esfahani, L. Roudaia, N. Buhlaiga, S. V. Del Rincon, N. Papneja, and W. H. Miller, “A review of cancer immunotherapy: From the past, to the present, to the future,” *Curr. Oncol.*, vol. 27, no. S2, pp. 87–97, 2020, doi: 10.3747/co.27.5223.

[22] S. A. Hussain, S. Williams, A. Stevens, and D. W. Rea, “Endocrine therapy for early breast cancer,” *Expert Rev. Anticancer Ther.*, vol. 4, no. 5, pp. 877–888, 2004, doi: 10.1586/14737140.4.5.877.

[23] S. Tohme, R. L. Simmons, and A. Tsung, “Surgery for cancer: A trigger for metastases,” *Cancer Res.*, vol. 77, no. 7, pp. 1548–1552, 2017, doi: 10.1158/0008-5472.CAN-16-1536.

[24] Routhier A *et al.*, "Pharmacological inhibition of Rho-kinase signaling with Y-27632 blocks melanoma tumor growth," *Oncol. Rep.*, vol. 23, no. 3, pp. 861–867, 2010, doi: 10.3892/or.

[25] N. G. Zaorsky, T. Allenby, J. Lin, J. Rosenberg, N. L. Simone, and K. H. Schmitz, "Exercise Therapy and Radiation Therapy for Cancer: A Systematic Review," *Int. J. Radiat. Oncol. Biol. Phys.*, vol. 110, no. 4, pp. 973–983, 2021, doi: 10.1016/j.ijrobp.2020.11.024.

[26] H. P. Kok, A. N. T. J. Kotte, and J. Crezee, "Planning, optimisation and evaluation of hyperthermia treatments," *Int. J. Hyperth.*, vol. 33, no. 6, pp. 593–607, Aug. 2017, doi: 10.1080/02656736.2017.1295323.

[27] "Hyperthermia to Treat Cancer," *American Cancer Society*. .

[28] M. Muscolini, E. Tassone, and J. Hiscott, "Oncolytic Immunotherapy: Can't Start a Fire Without a Spark," *Cytokine Growth Factor Rev.*, vol. 56, no. July, pp. 94–101, 2020, doi: 10.1016/j.cytogfr.2020.07.014.

[29] "Immunotherapy," *American ancer Society*. .

[30] A. Mandal, "Que é metástase?," *News medical life sciences*. .

[31] J. J. G. Marin, M. R. Romero, A. G. Blazquez, E. Herraez, E. Keck, and O. Briz, "Importance and Limitations of Chemotherapy Among the Available Treatments for Gastrointestinal Tumours," *Anticancer. Agents Med. Chem.*, vol. 9, no. 2, pp. 162–184, 2012, doi: 10.2174/187152009787313828.

[32] R. Baskar, K. A. Lee, R. Yeo, and K. W. Yeoh, "Cancer and radiation therapy: Current advances and future directions," *Int. J. Med. Sci.*, vol. 9, no. 3, pp. 193–199, 2012, doi: 10.7150/ijms.3635.

[33] J. W. Snider, N. R. Datta, and Z. Vujaskovic, "Hyperthermia and radiotherapy in bladder cancer," *International Journal of Hyperthermia*, vol. 32, no. 4. Taylor and Francis Ltd, pp. 398–406, May 2016, doi: 10.3109/02656736.2016.1150524.

[34] "Hyperthermia to Treat Cancer," *National Cancer Institute*. .

[35] M. Pavel and A. Stancu, "Ferromagnetic nanoparticles dose based on tumor size in magnetic fluid hyperthermia cancer therapy," in *IEEE Transactions on Magnetics*, Nov. 2009, vol. 45, no. 11, pp. 5251–5254, doi: 10.1109/TMAG.2009.2031076.

[36] D. Chang *et al.*, "Biologically targeted magnetic hyperthermia: Potential and limitations," *Frontiers in Pharmacology*, vol. 9, no. AUG. Frontiers Media S.A., Aug. 2018, doi:

10.3389/fphar.2018.00831.

[37] N. H. Andra W, *Magnetism in Medicine: A Handbook*, First ed. Germany: Wiley-VCH, 1998.

[38] M. C. Tan, *Nanostructured materials for biomedical applications*. Transworld research network, 2009.

[39] A. Jordan, P. Wust, H. Fahling, W. Johns, A. Hinzt, and R. Felix, "Inductive heating of ferrimagnetic particles and magnetic fluids: physical evaluation of their potential for hyperthermia," 1993.

[40] V. F. Cardoso, A. Francesko, C. Ribeiro, M. Bañobre-López, P. Martins, and S. Lanceros-Mendez, "Advances in Magnetic Nanoparticles for Biomedical Applications," *Advanced Healthcare Materials*, vol. 7, no. 5. Wiley-VCH Verlag, Mar. 2018, doi: 10.1002/adhm.201700845.

[41] E. A. Périgo *et al.*, "Fundamentals and advances in magnetic hyperthermia," *Applied Physics Reviews*, vol. 2, no. 4. American Institute of Physics Inc., Dec. 2015, doi: 10.1063/1.4935688.

[42] J. Yang *et al.*, "Multifunctional magneto-polymeric nanohybrids for targeted detection and synergistic therapeutic effects on breast cancer," *Angew. Chemie - Int. Ed.*, vol. 46, no. 46, pp. 8836–8839, 2007, doi: 10.1002/anie.200703554.

[43] S. Chandra Mohanta, A. Saha, and P. Sujatha Devi, "PEGylated Iron Oxide Nanoparticles for pH Responsive Drug Delivery Application," 2018.

[44] P. C. Liang *et al.*, "Doxorubicin-modified magnetic nanoparticles as a drug delivery system for magnetic resonance imaging-monitoring magnet-enhancing tumor chemotherapy," *Int. J. Nanomedicine*, vol. 11, pp. 2021–2037, May 2016, doi: 10.2147/IJN.S94139.

[45] M. Levy *et al.*, "Correlating magneto-structural properties to hyperthermia performance of highly monodisperse iron oxide nanoparticles prepared by a seeded-growth route," *Chem. Mater.*, vol. 23, no. 18, pp. 4170–4180, Sep. 2011, doi: 10.1021/cm201078f.

[46] M. Taupitz, S. Wagner, B. Hamm, D. Dienemann, R. Lawaczeck, and K.-J. Wolf, "MR Lymphography Using Iron Oxide Particles," *Acta radiol.*, vol. 34, no. 1, pp. 10–15, Jan. 1993, doi: 10.1080/02841859309173228.

[47] M. G. Harisinghani *et al.*, "Noninvasive Detection of Clinically Occult Lymph-Node Metastases in Prostate Cancer," 2003.

[48] S. Majidi *et al.*, "Magnetic nanoparticles: Applications in gene delivery and gene therapy,"

Artif. Cells, Nanomedicine Biotechnol., vol. 44, no. 4, pp. 1186–1193, May 2016, doi: 10.3109/21691401.2015.1014093.

[49] M. Pavlin, D. Zupančič, J. Lojk, K. Strojan, and M. E. Kreft, "Multimodal magnetic nanoparticles for biomedical applications: Importance of characterization on biomimetic in vitro models," in *Materials for Biomedical Engineering: Inorganic Micro- and Nanostructures*, Elsevier, 2019, pp. 241–283.

[50] E. Vedmedenko, *Competing Interactions and Patterns in Nanoworld The Chemistry of Nanomaterials Nanoparticles Introduction to Nanotechnology*. 2007.

[51] T. Kobayashi, "Cancer hyperthermia using magnetic nanoparticles," *Biotechnol. J.*, vol. 6, no. 11, pp. 1342–1347, 2011, doi: 10.1002/biot.201100045.

[52] C. Bárcena, A. K. Sra, and J. Gao, "Applications of magnetic nanoparticles in biomedicine," *Nanoscale Magn. Mater. Appl.*, vol. 167, pp. 591–626, 2009, doi: 10.1007/978-0-387-85600-1_20.

[53] T. Atsumi, B. Jeyadevan, Y. Sato, and K. Tohji, "Fundamental Approach for a Cancer Therapy Method Using Magnetic Particles as Thermo-seeds 1 : Development of Magnetic Particles Suitable for Hyperthermia," *J. Magn. Soc. Japan*, vol. 30, no. 6, pp. 555–560, 2006.

[54] T. Atsumi, B. Jeyadevan, Y. Sato, and K. Tohji, "Heating efficiency of magnetite particles exposed to AC magnetic field," *J. Magn. Magn. Mater.*, vol. 310, no. 2 SUPPL. PART 3, pp. 2841–2843, 2007, doi: 10.1016/j.jmmm.2006.11.063.

[55] C. Sun, J. S. H. Lee, and M. Zhang, "Magnetic nanoparticles in MR imaging and drug delivery," *Advanced Drug Delivery Reviews*, vol. 60, no. 11. pp. 1252–1265, Aug. 2008, doi: 10.1016/j.addr.2008.03.018.

[56] P. Tartaj, M. Del Puerto Morales, S. Veintemillas-Verdaguer, T. González-Carreño, C. Carreño, and C. J. Serna, "The preparation of magnetic nanoparticles for applications in biomedicine," 2003.

[57] U. S. Johansson, J. Fjeldså, and R. C. K. Bowie, "Phylogenetic relationships within Passerida (Aves: Passeriformes): A review and a new molecular phylogeny based on three nuclear intron markers," *Mol. Phylogenet. Evol.*, vol. 48, no. 3, pp. 858–876, Sep. 2008, doi: 10.1016/j.ympev.2008.05.029.

[58] L. Lartigue *et al.*, "Water-dispersible sugar-coated iron oxide nanoparticles. An evaluation of their relaxometric and magnetic hyperthermia properties," *J. Am. Chem. Soc.*, vol.

133, no. 27, pp. 10459–10472, Jul. 2011, doi: 10.1021/ja111448t.

[59] F. Mohammad, G. Balaji, A. Weber, R. M. Uppu, and C. S. S. R. Kumar, "Influence of gold nanoshell on hyperthermia of superparamagnetic iron oxide nanoparticles," *J. Phys. Chem. C*, vol. 114, no. 45, pp. 19194–19201, Nov. 2010, doi: 10.1021/jp105807r.

[60] D. L. Zhao, H. L. Zhang, X. W. Zeng, Q. S. Xia, and J. T. Tang, "Inductive heat property of Fe3O4/polymer composite nanoparticles in an ac magnetic field for localized hyperthermia," *Biomed. Mater.*, vol. 1, no. 4, pp. 198–201, 2006, doi: 10.1088/1748-6041/1/4/004.

[61] G. Zhang, Y. Liao, and I. Baker, "Surface engineering of core/shell iron/iron oxide nanoparticles from microemulsions for hyperthermia," *Mater. Sci. Eng. C*, vol. 30, no. 1, pp. 92–97, Jan. 2010, doi: 10.1016/j.msec.2009.09.003.

[62] V. Patsula *et al.*, "Superparamagnetic Fe3O4 Nanoparticles: Synthesis by Thermal Decomposition of Iron(III) Glucuronate and Application in Magnetic Resonance Imaging," *ACS Appl. Mater. Interfaces*, vol. 8, no. 11, pp. 7238–7247, 2016, doi: 10.1021/acsami.5b12720.

[63] S. Nigam, K. C. Barick, and D. Bahadur, "Development of citrate-stabilized Fe3O4 nanoparticles: Conjugation and release of doxorubicin for therapeutic applications," *J. Magn. Magn. Mater.*, vol. 323, no. 2, pp. 237–243, Jan. 2011, doi: 10.1016/j.jmmm.2010.09.009.

[64] L. A. Thomas *et al.*, "Carboxylic acid-stabilised iron oxide nanoparticles for use in magnetic hyperthermia," *J. Mater. Chem.*, vol. 19, no. 36, pp. 6529–6535, 2009, doi: 10.1039/b908187a.

[65] J. Jose *et al.*, "Magnetic nanoparticles for hyperthermia in cancer treatment: an emerging tool," *Environ. Sci. Pollut. Res.*, vol. 27, no. 16, pp. 19214–19225, 2020, doi: 10.1007/s11356-019-07231-2.

[66] R. V. Ferreira, "Universidade Federal de Minas Gerais Instituto de Ciências Exatas Departamento de Química Roberta Viana Ferreira Síntese e Caracterização de Nanopartículas Magnéticas Funcionalizadas com Núcleo Magnético de Magnetita Belo Horizonte Síntese e Caracterizaçã," 2009.

[67] S. M. Roy and S. K. Sahoo, "Controlled Drug Delivery: Polymeric Biomaterials for," *Encycl. Biomed. Polym. Polym. Biomater.*, no. January, pp. 2135–2146, 2016, doi: 10.1081/e-ebpp-120050023.

[68] R. De Souza, P. Zahedi, C. J. Allen, and M. Piquette-Miller, "Polymeric drug delivery systems for localized cancer chemotherapy," *Drug Deliv.*, vol. 17, no. 6, pp. 365–375, 2010, doi: 10.3109/10717541003762854.

[69] G. Tiwari *et al.*, "Drug delivery systems: An updated review," *Int. J. Pharm. Investig.*, vol. 2, no. 1, p. 2, 2012, doi: 10.4103/2230-973x.96920.

[70] E. J. Torres-Martinez, J. M. Cornejo Bravo, A. Serrano Medina, G. L. Pérez González, and L. J. Villarreal Gómez, "A Summary of Electrospun Nanofibers as Drug Delivery System: Drugs Loaded and Biopolymers Used as Matrices," *Curr. Drug Deliv.*, vol. 15, no. 10, pp. 1360–1374, 2018, doi: 10.2174/1567201815666180723114326.

[71] F. Sharifi, A. C. Sooriyarachchi, H. Altural, R. Montazami, M. N. Rylander, and N. Hashemi, "Fiber Based Approaches as Medicine Delivery Systems," *ACS Biomater. Sci. Eng.*, vol. 2, no. 9, pp. 1411–1431, 2016, doi: 10.1021/acsbiomaterials.6b00281.

[72] S. Y. Ahn, C. H. Mun, and S. H. Lee, *Microfluidic spinning of fibrous alginate carrier having highly enhanced drug loading capability and delayed release profile*, vol. 5, no. 20. 2015.

[73] D. Chen, D. Singh, K. K. Sirkar, and R. Pfeffer, "Continuous synthesis of polymer-coated drug particles by porous hollow fiber membrane-based antisolvent crystallization," *Langmuir*, vol. 31, no. 1, pp. 432–441, 2015, doi: 10.1021/la503179t.

[74] T. Garg, G. Rath, and A. K. Goyal, "Biomaterials-based nanofiber scaffold: Targeted and controlled carrier for cell and drug delivery," *J. Drug Target.*, vol. 23, no. 3, pp. 202–221, 2015, doi: 10.3109/1061186X.2014.992899.

[75] J. G. Fernandes *et al.*, "PHB-PEO electrospun fiber membranes containing chlorhexidine for drug delivery applications," *Polym. Test.*, vol. 34, pp. 64–71, 2014, doi: 10.1016/j.polymertesting.2013.12.007.

[76] H. L. Nie *et al.*, "Polyacrylonitrile fibers efficiently loaded with tamoxifen citrate using wet-spinning from co-dissolving solution," *Int. J. Pharm.*, vol. 373, no. 1–2, pp. 4–9, 2009, doi: 10.1016/j.ijpharm.2009.03.022.

[77] E. R. Kenawy, F. I. Abdel-Hay, M. H. El-Newehy, and G. E. Wnek, "Processing of polymer nanofibers through electrospinning as drug delivery systems," *Mater. Chem. Phys.*, vol. 113, no. 1, pp. 296–302, 2009, doi: 10.1016/j.matchemphys.2008.07.081.

[78] L. Wang, M. W. Chang, Z. Ahmad, H. Zheng, and J. S. Li, "Mass and controlled fabrication of aligned PVP fibers for matrix type antibiotic drug delivery systems," *Chem.*

Eng. J., vol. 307, pp. 661–669, 2017, doi: 10.1016/j.cej.2016.08.135.

[79] J. Zeng *et al.*, "Biodegradable electrospun fibers for drug delivery," *J. Control. Release*, vol. 92, no. 3, pp. 227–231, 2003, doi: 10.1016/S0168-3659(03)00372-9.

[80] D. G. Yu, X. X. Shen, Y. Zheng, Z. H. Ma, L. M. Zhu, and C. Branford-White, "Wet-spinning medicated PAN/PCL fibers for drug sustained release," *2nd Int. Conf. Bioinforma. Biomed. Eng. iCBBE 2008*, pp. 1375–1378, 2008, doi: 10.1109/ICBBE.2008.673.

[81] L. Liu, L. Jiang, G. K. Xu, C. Ma, X. G. Yang, and J. M. Yao, "Potential of alginate fibers incorporated with drug-loaded nanocapsules as drug delivery systems," *J. Mater. Chem. B*, vol. 2, no. 43, pp. 7596–7604, 2014, doi: 10.1039/c4tb01392a.

[82] S. J. Wade *et al.*, "Preparation and in vitro assessment of wet-spun gemcitabine-loaded polymeric fibers: Towards localized drug delivery for the treatment of pancreatic cancer," *Pancreatology*, vol. 17, no. 5, pp. 795–804, 2017, doi: 10.1016/j.pan.2017.06.001.

[83] J. Ding, Y. Bu, M. Ou, Y. Yu, Q. Zhong, and M. Fan, "Facile decoration of carbon fibers with Ag nanoparticles for adsorption and photocatalytic reduction of CO2," *Appl. Catal. B Environ.*, vol. 202, pp. 314–325, 2017, doi: 10.1016/j.apcatb.2016.09.038.

[84] D. Wawro and L. Pighinelli, "Chitosan fibers modified with HAp/β-TCP nanoparticles," *Int. J. Mol. Sci.*, vol. 12, no. 11, pp. 7286–7300, 2011, doi: 10.3390/ijms12117286.

[85] E. Smiechowicz, P. Kulpinski, B. Niekraszewicz, and A. Bacciarelli, "Cellulose fibers modified with silver nanoparticles," *Cellulose*, vol. 18, no. 4, pp. 975–985, 2011, doi: 10.1007/s10570-011-9544-9.

[86] H. Dong, A. Meininger, H. Jiang, K. S. Moon, and C. P. Wong, "Magnetic nanocomposite for potential ultrahigh frequency microelectronic application," *J. Electron. Mater.*, vol. 36, no. 5, pp. 593–597, 2007, doi: 10.1007/s11664-007-0112-x.

[87] M. Wang, H. Singh, T. A. Hatton, and G. C. Rutledge, "Field-responsive superparamagnetic composite nanofibers by electrospinning," *Polymer (Guildf).*, vol. 45, no. 16, pp. 5505–5514, 2004, doi: 10.1016/j.polymer.2004.06.013.

[88] R. L. Andersson, L. Cabedo, M. S. Hedenqvist, R. T. Olsson, and V. Ström, "Superparamagnetic [sic] nanofibers by electrospinning," *RSC Adv.*, vol. 6, no. 26, pp. 21413–21422, 2016, doi: 10.1039/c5ra27791d.

[89] L. Chen, N. Fujisawa, M. Takanohashi, M. Najmina, K. Uto, and M. Ebara, "A smart hyperthermia nanofiber-platform-enabled sustained release of doxorubicin and 17aag for synergistic cancer therapy," *Int. J. Mol. Sci.*, vol. 22, no. 5, pp. 1–11, 2021, doi:

10.3390/ijms22052542.

[90] P. Tiwari, S. Agarwal, S. Srivastava, and S. Jain, "The combined effect of thermal and chemotherapy on HeLa cells using magnetically actuated smart textured fibrous system," *J. Biomed. Mater. Res. - Part B Appl. Biomater.*, vol. 106, no. 1, pp. 40–51, 2018, doi: 10.1002/jbm.b.33812.

[91] A. R. K. Sasikala, A. R. Unnithan, Y. H. Yun, C. H. Park, and C. S. Kim, "An implantable smart magnetic nanofiber device for endoscopic hyperthermia treatment and tumor-triggered controlled drug release," *Acta Biomater.*, vol. 31, pp. 122–133, 2016, doi: 10.1016/j.actbio.2015.12.015.

[92] Y. J. Kim, M. Ebara, and T. Aoyagi, "A smart hyperthermia nanofiber with switchable drug release for inducing cancer apoptosis," *Adv. Funct. Mater.*, vol. 23, no. 46, pp. 5753–5761, 2013, doi: 10.1002/adfm.201300746.

[93] T. C. Lin, F. H. Lin, and J. C. Lin, "In vitro characterization of magnetic electrospun IDA-grafted chitosan nanofiber composite for hyperthermic tumor cell treatment," *J. Biomater. Sci. Polym. Ed.*, vol. 24, no. 9, pp. 1152–1163, 2013, doi: 10.1080/09205063.2012.743061.

[94] K. A. Van Kampen *et al.*, *Biofabrication: From additive manufacturing to bioprinting*, vol. 1–3. Elsevier Inc., 2019.

[95] E. A. Aksoy *et al.*, "Vancomycin Loaded Gelatin Microspheres Containing Wet Spun Poly(ε-caprolactone) Fibers and Films for Osteomyelitis Treatment," *Fibers Polym.*, vol. 20, no. 11, pp. 2236–2246, 2019, doi: 10.1007/s12221-019-9271-7.

[96] M. T. Arafat, G. Tronci, D. J. Wood, and S. J. Russell, "In-situ crosslinked wet spun collagen triple helices with nanoscale-regulated ciprofloxacin release capability," *Mater. Lett.*, vol. 255, p. 126550, 2019, doi: 10.1016/j.matlet.2019.126550.

[97] B. Singhi, E. N. Ford, and M. W. King, "The effect of wet spinning conditions on the structure and properties of poly-4-hydroxybutyrate fibers," *J. Biomed. Mater. Res. - Part B Appl. Biomater.*, vol. 109, no. 7, pp. 982–989, 2021, doi: 10.1002/jbm.b.34763.

[98] D. G. Yu, X. X. Shen, L. M. Zhu, C. Branford-White, S. W. Annie Bligh, and Y. C. Yang, "Preparation and characterization of medicated PAN/PVP composite fibers for better drug release profiles," *3rd Int. Conf. Bioinforma. Biomed. Eng. iCBBE 2009*, pp. 2–5, 2009, doi: 10.1109/ICBBE.2009.5163228.

[99] H. Uğuz *et al.*, "Fabrication and characterization of biopolymer fibers for 3D oriented

microvascular structures," *J. Phys. Energy*, vol. 2, no. 1, pp. 0–31, 2020.

[100] A. B. Balaji, H. Pakalapati, M. Khalid, R. Walvekar, and H. Siddiqui, *Natural and synthetic biocompatible and biodegradable polymers*. Elsevier Ltd, 2017.

[101] K. Kalantari, A. M. Afifi, H. Jahangirian, and T. J. Webster, "Biomedical applications of chitosan electrospun nanofibers as a green polymer – Review," *Carbohydr. Polym.*, vol. 207, pp. 588–600, 2019, doi: 10.1016/j.carbpol.2018.12.011.

[102] A. Muxika, A. Etxabide, J. Uranga, P. Guerrero, and K. de la Caba, "Chitosan as a bioactive polymer: Processing, properties and applications," *Int. J. Biol. Macromol.*, vol. 105, pp. 1358–1368, 2017, doi: 10.1016/j.ijbiomac.2017.07.087.

[103] B. Das and S. Patra, *Antimicrobials: Meeting the Challenges of Antibiotic Resistance Through Nanotechnology*. Elsevier Inc., 2017.

[104] C. L. Ke, F. S. Deng, C. Y. Chuang, and C. H. Lin, "Antimicrobial actions and applications of Chitosan," *Polymers (Basel).*, vol. 13, no. 6, 2021, doi: 10.3390/polym13060904.

[105] G. C. East and Y. Qin, "Wet spinning of chitosan and the acetylation of chitosan fibers," *J. Appl. Polym. Sci.*, vol. 50, no. 10, pp. 1773–1779, 1993, doi: 10.1002/app.1993.070501013.

[106] J. Brugnerotto, J. Desbrières, L. Heux, K. Mazeau, and M. Rinaudo, "Wet-spinning and applications of functional fibers based on chitin and chitosan," *Macromol. Symp.*, vol. 168, pp. 21–30, 2001, doi: 10.1002/1521-3900(200103)168:1<21::AID-MASY21>3.0.CO;2-D.

[107] C. A. Vega-Cázarez, J. López-Cervantes, D. I. Sánchez-Machado, T. J. Madera-Santana, A. Soto-Cota, and B. Ramírez-Wong, "Preparation and Properties of Chitosan–PVA Fibers Produced by Wet Spinning," *J. Polym. Environ.*, vol. 26, no. 3, pp. 946–958, 2018, doi: 10.1007/s10924-017-1003-8.

[108] A. Subramanian and H. Y. Lin, "Crosslinked chitosan: Its physical properties and the effects of matrix stiffness on chondrocyte cell morphology and proliferation," *J. Biomed. Mater. Res. - Part A*, vol. 75, no. 3, pp. 742–753, 2005, doi: 10.1002/jbm.a.30489.

[109] C. G. T. Neto, T. N. C. Dantas, J. L. C. Fonseca, and M. R. Pereira, "Permeability studies in chitosan membranes. Effects of crosslinking and poly(ethylene oxide) addition," *Carbohydr. Res.*, vol. 340, no. 17, pp. 2630–2636, 2005, doi: 10.1016/j.carres.2005.09.011.

[110] G. C. Ritthidej, T. Phaechamud, and T. Koizumi, "Moist heat treatment on

physicochemical change of chitosan salt films," *Int. J. Pharm.*, vol. 232, no. 1–2, pp. 11–22, 2002, doi: 10.1016/S0378-5173(01)00894-8.

[111] J. D. Schiffman and C. L. Schauer, "Cross-linking chitosan nanofibers," *Biomacromolecules*, vol. 8, no. 2, pp. 594–601, 2007, doi: 10.1021/bm060804s.

[112] A. H. Jawad and M. A. Nawi, "Oxidation of crosslinked chitosan-epichlorohydrine film and its application with TiO 2 for phenol removal," *Carbohydr. Polym.*, vol. 90, no. 1, pp. 87–94, 2012, doi: 10.1016/j.carbpol.2012.04.066.

[113] Z. Yang, H. Peng, W. Wang, and T. Liu, "Crystallization behavior of poly(ε-caprolactone)/layered double hydroxide nanocomposites," *J. Appl. Polym. Sci.*, vol. 116, no. 5, pp. 2658–2667, 2010, doi: 10.1002/app.

[114] F. Kalalinia *et al.*, "Evaluation of wound healing efficiency of vancomycin-loaded electrospun chitosan/poly ethylene oxide nanofibers in full thickness wound model of rat," *Int. J. Biol. Macromol.*, vol. 177, pp. 100–110, 2021, doi: 10.1016/j.ijbiomac.2021.01.209.

[115] S. H. Lee, S. Y. Park, and J. H. Choi, "Fiber formation and physical properties of chitosan fiber crosslinked by epichlorohydrin in a wet spinning system: The effect of the concentration of the crosslinking agent epichlorohydrin," *J. Appl. Polym. Sci.*, vol. 92, no. 3, pp. 2054–2062, 2004, doi: 10.1002/app.20160.

[116] M. Y. Kariduraganavar, A. A. Kittur, and R. R. Kamble, *Polymer Synthesis and Processing*, 1st ed. Elsevier Inc., 2014.

[117] R. B. Lima, "Nanofibras de Materiais Biológicos," 2013.

[118] S. Abid *et al.*, "Enhanced antibacterial activity of PEO-chitosan nanofibers with potential application in burn infection management," *Int. J. Biol. Macromol.*, vol. 135, pp. 1222–1236, 2019, doi: 10.1016/j.ijbiomac.2019.06.022.

[119] G. Ma, Y. Liu, C. Peng, D. Fang, B. He, and J. Nie, "Paclitaxel loaded electrospun porous nanofibers as mat potential application for chemotherapy against prostate cancer," *Carbohydr. Polym.*, vol. 86, no. 2, pp. 505–512, 2011, doi: 10.1016/j.carbpol.2011.04.082.

[120] M. Rahimi, A. Jafari, S. J. S. Tabaei, M. Rahimi, S. Taranejoo, and M. Ghanimatdan, "Herbal Extract Incorporated Chitosan Based Nanofibers as a New Strategy for Smart Anticancer Drug Delivery System: An In Vitro Model," *Worl Cancer Res. J.*, vol. 7, no. 0, pp. 1–11, 2020.

[121] B. K. Tan, Y. C. Ching, S. C. Poh, L. C. Abdullah, and S. N. Gan, "A review of natural fiber reinforced poly(vinyl alcohol) based composites: Application and opportunity," *Polymers (Basel).*, vol. 7, no. 11, pp. 2205–2222, 2015, doi: 10.3390/polym7111509.

[122] K. T. Shalumon *et al.*, "Electrospinning of carboxymethyl chitin/poly(vinyl alcohol) nanofibrous scaffolds for tissue engineering applications," *Carbohydr. Polym.*, vol. 77, no. 4, pp. 863–869, 2009, doi: 10.1016/j.carbpol.2009.03.009.

[123] E. Yan *et al.*, "Biocompatible core-shell electrospun nanofibers as potential application for chemotherapy against ovary cancer," *Mater. Sci. Eng. C*, vol. 41, pp. 217–223, 2014, doi: 10.1016/j.msec.2014.04.053.

[124] E. Yan *et al.*, "Polycaprolactone/polyvinyl alcohol core-shell nanofibers as a pH-responsive drug carrier for the potential application in chemotherapy against colon cancer," *Mater. Lett.*, vol. 291, p. 129516, 2021, doi: 10.1016/j.matlet.2021.129516.

[125] S. S. Qavamnia, L. R. Rad, and M. Irani, "Incorporation of Hydroxyapatite/Doxorubicin into the Chitosan/Polyvinyl Alcohol/Polyurethane Nanofibers for Controlled Release of Doxurubicin and Its Anticancer Property," *Fibers Polym.*, vol. 21, no. 8, pp. 1634–1642, 2020, doi: 10.1007/s12221-020-9809-8.

[126] C. A. Henriques, A. Fernandes, L. M. Rossi, M. F. Ribeiro, M. J. F. Calvete, and M. M. Pereira, "Biologically Inspired and Magnetically Recoverable Copper Porphyrinic Catalysts: A Greener Approach for Oxidation of Hydrocarbons with Molecular Oxygen," *Adv. Funct. Mater.*, vol. 26, no. 19, pp. 3359–3368, 2016, doi: 10.1002/adfm.201505405.

[127] H. M. Ng, N. M. Saidi, F. S. Omar, K. Ramesh, S. Ramesh, and S. Bashir, "Thermogravimetric Analysis of Polymers," *Encycl. Polym. Sci. Technol.*, no. 13, pp. 1–29, 2018, doi: 10.1002/0471440264.pst667.

[128] A. S. Ribeiro *et al.*, "Chitosan/nanocellulose electrospun fibers with enhanced antibacterial and antifungal activity for wound dressing applications," *React. Funct. Polym.*, vol. 159, no. September 2020, 2021, doi: 10.1016/j.reactfunctpolym.2020.104808.

[129] J. Guo, X. Ye, W. Liu, Q. Wu, H. Shen, and K. Shu, "Preparation and characterization of poly(acrylonitrile-co-acrylic acid) nanofibrous composites with Fe3O4 magnetic nanoparticles," *Mater. Lett.*, vol. 63, no. 15, pp. 1326–1328, 2009, doi: 10.1016/j.matlet.2009.02.068.

[130] S. Wang *et al.*, "Magnetic composite nanofibers fabricated by electrospinning of

Fe3O4/gelatin aqueous solutions," *Mater. Sci. Eng. B Solid-State Mater. Adv. Technol.*, vol. 190, pp. 126–132, 2014, doi: 10.1016/j.mseb.2014.10.001.

[131] S. Nigam, K. C. Barick, and D. Bahadur, "Development of citrate-stabilized Fe3O4 nanoparticles: Conjugation and release of doxorubicin for therapeutic applications," *J. Magn. Magn. Mater.*, vol. 323, no. 2, pp. 237–243, 2011, doi: 10.1016/j.jmmm.2010.09.009.

[132] D. Brüggemann, J. Michel, N. Suter, M. G. de Aguiar, and M. Maas, "Wet-spinning of magneto-responsive helical chitosan microfibers," *Beilstein J. Nanotechnol.*, vol. 11, pp. 991–999, 2020, doi: 10.3762/bjnano.11.83.

[133] P. Chen, L. Liu, J. Pan, J. Mei, C. Li, and Y. Zheng, "Biomimetic composite scaffold of hydroxyapatite/gelatin-chitosan core-shell nanofibers for bone tissue engineering," *Mater. Sci. Eng. C*, vol. 97, pp. 325–335, 2019, doi: 10.1016/j.msec.2018.12.027.

[134] L. Deng *et al.*, *Electrospun Chitosan/Poly(ethylene oxide)/Lauric Arginate Nanofibrous Film with Enhanced Antimicrobial Activity*, vol. 66, no. 24. 2018.

[135] V. Vijayalekshmi and D. Khastgir, "Eco-friendly methanesulfonic acid and sodium salt of dodecylbenzene sulfonic acid doped cross-linked chitosan based green polymer electrolyte membranes for fuel cell applications," *J. Memb. Sci.*, vol. 523, pp. 45–59, 2017, doi: 10.1016/j.memsci.2016.09.058.

[136] K. Jalaja, D. Naskar, S. C. Kundu, and N. R. James, "Potential of electrospun core-shell structured gelatin-chitosan nanofibers for biomedical applications," *Carbohydr. Polym.*, vol. 136, pp. 1098–1107, 2016, doi: 10.1016/j.carbpol.2015.10.014.

[137] N. Cai *et al.*, "Tailoring mechanical and antibacterial properties of chitosan/gelatin nanofiber membranes with Fe 3 O 4 nanoparticles for potential wound dressing application," *Appl. Surf. Sci.*, vol. 369, pp. 492–500, 2016, doi: 10.1016/j.apsusc.2016.02.053.

[138] P. Kianfar, A. Vitale, S. Dalle Vacche, and R. Bongiovanni, "Photo-crosslinking of chitosan/poly(ethylene oxide) electrospun nanofibers," *Carbohydr. Polym.*, vol. 217, pp. 144–151, 2019, doi: 10.1016/j.carbpol.2019.04.062.

[139] M. Pakravan, M. C. Heuzey, and A. Ajji, "A fundamental study of chitosan/PEO electrospinning," *Polymer (Guildf).*, vol. 52, no. 21, pp. 4813–4824, 2011, doi: 10.1016/j.polymer.2011.08.034.

[140] F. Tasselli, A. Mirmohseni, M. S. Seyed Dorraji, and A. Figoli, "Mechanical, swelling and

adsorptive properties of dry-wet spun chitosan hollow fibers crosslinked with glutaraldehyde," *React. Funct. Polym.*, vol. 73, no. 1, pp. 218–223, 2013, doi: 10.1016/j.reactfunctpolym.2012.08.007.

[141] S. Fathollahipour, A. Abouei Mehrizi, A. Ghaee, and M. Koosha, "Electrospinning of PVA/chitosan nanocomposite nanofibers containing gelatin nanoparticles as a dual drug delivery system," *J. Biomed. Mater. Res. - Part A*, vol. 103, no. 12, pp. 3852–3862, 2015, doi: 10.1002/jbm.a.35529.

[142] K. Tuzlakoglu, C. M. Alves, J. F. Mano, and R. L. Reis, "Production and characterization of chitosan fibers and 3-D fiber mesh scaffolds for tissue engineering applications," *Macromol. Biosci.*, vol. 4, no. 8, pp. 811–819, 2004, doi: 10.1002/mabi.200300100.

[143] S. S. Davis, "Biomedical applications of nanotechnology - implications for drug targeting and gene therapy," *Trends Biotechnol.*, vol. 15, no. 6, pp. 217–224, 1997, doi: 10.1016/S0167-7799(97)01036-6.

[144] A. J. Cole, A. E. David, J. Wang, C. J. Galbán, and V. C. Yang, "Magnetic brain tumor targeting and biodistribution of long-circulating PEG-modified, cross-linked starch-coated iron oxide nanoparticles," *Biomaterials*, vol. 32, no. 26, pp. 6291–6301, 2011, doi: 10.1016/j.biomaterials.2011.05.024.